UC Davis
Research Reports

Title
Impact of Silo Storage on the Performance of Plant-Produced Mixes Containing High Content of Reclaimed Asphalt Pavement or Reclaimed Asphalt Shingles

Permalink
https://escholarship.org/uc/item/24p1v6fd

Authors
Elkashef, Mohamed
Harvey, John
Jiao, Liya
et al.

Publication Date
2023-02-01

DOI
10.7922/G24J0CFF

Impact of Silo Storage on the Performance of Plant-Produced Mixes Containing High Content of Reclaimed Asphalt Pavement or Reclaimed Asphalt Shingles

Authors:

Mohamed Elkashef, John Harvey, Liya Jiao, David Jones

PREPARED FOR:

California Department of Transportation
Division of Research, Innovation, and System Information
Office of Materials and Infrastructure

PREPARED BY:

University of California
Pavement Research Center
UC Davis, UC Berkeley

TECHNICAL REPORT DOCUMENTATION PAGE

1. REPORT NUMBER UCPRC-RR-2022-04	2. GOVERNMENT ASSOCIATION NUMBER	3. RECIPIENT'S CATALOG NUMBER
4. TITLE AND SUBTITLE Impact of Silo Storage on the Performance of Plant-Produced Mixes Containing High Content of Reclaimed Asphalt Pavement and Reclaimed Asphalt Shingles		5. REPORT PUBLICATION DATE February 2023
		6. PERFORMING ORGANIZATION CODE
7. AUTHOR(S) Mohamed Elkashef (ORCID 0000-0002-8028-1935), John Harvey (ORCID 0000-0002-8924-6212) Liya Jiao (ORCID 0000-0003-0648-693X), and David Jones (ORCID 0000-0002-2938-076X)		8. PERFORMING ORGANIZATION REPORT NO. UCPRC-RR-2022-04 UCD-ITS-RR-22-125
9. PERFORMING ORGANIZATION NAME AND ADDRESS University of California Pavement Research Center Department of Civil and Environmental Engineering, UC Davis 1 Shields Avenue Davis, CA 95616		10. WORK UNIT NUMBER
		11. CONTRACT OR GRANT NUMBER 4.64
12. SPONSORING AGENCY AND ADDRESS California Department of Transportation Division of Research, Innovation, and System Information P.O. Box 942873 Sacramento, CA 94273-0001		13. TYPE OF REPORT AND PERIOD COVERED Research Report July 2018 to May 2022
		14. SPONSORING AGENCY CODE

16. ABSTRACT

Use of recycled materials, such as reclaimed asphalt pavement (RAP) and reclaimed asphalt shingles (RAS), is gaining widespread interest. Currently the California Department of Transportation standard specifications do not allow the use of RAS and limit the use of RAP contents to a maximum of 25% by dry weight of aggregate, though there is a non-standard special provision that allows use of up to 3% RAS by mass of aggregate and 40% RAP content by binder replacement. Nevertheless, mixes with high RAP and RAS are being produced across California for local agencies and commercial use. This study investigated the performance of four plant-produced high RAP or RAS mixes collected from different regions in California. The mixes were not designed and produced following Caltrans specifications. However, they provide insight into the effects of silo storage time on blending of virgin and RAP binder, the performance-related properties of these mixes, and the measurement of properties by accepted performance-related tests. The mixes were collected before silo storage and after hours in the silo. Testing of the mixes included the following tests: four-point flexural beam stiffness and fatigue, Hamburg Wheel-Track (HWT), confined and unconfined repeated load triaxial (RLT), semicircular bending (SCB), and indirect tensile asphalt cracking test (IDEAL-CT). Additional testing was also conducted on the fine aggregate matrix (FAM) mixes to characterize fatigue and stiffness. This report presents preliminary findings from this study, including results related to the effects of silo storage time on stiffness, cracking resistance, and rutting resistance using performance-related tests as well as an initial comparison of the results from alternative cracking test types for these mixes. The results showed that silo storage time can increase stiffness on the order of 50% to 60%, with corresponding negative effects on fracture resistance and controlled-strain flexural fatigue life. The fatigue performance of the mixes reduced with increased silo storage, particularly at high strain levels, as measured by the flexural beam test. Use of a high rejuvenator dose could also potentially lead to rutting problems and poor fatigue performance. The FAM mix testing showed promising results in terms of characterizing fatigue. However, in its current form, it is not yet practical for use as a quality control/quality assurance test. The recommendation is that the effect of aging and blending of high RAP or RAS mixes be further investigated to understand the full impact of silo storage on these types of mixes. Performance-related specifications should consider the variation in mix properties due to silo storage.

| 17. KEY WORDS
reclaimed asphalt pavement, reclaimed asphalt shingles, recycled asphalt, asphalt aging, short-term aging, silo storage, performance-related testing, rutting; cracking, fatigue | 18. DISTRIBUTION STATEMENT

No restrictions. This document is available to the public through the National Technical Information Service, Springfield, VA 22161 | |
| 19. SECURITY CLASSIFICATION (of this report)

Unclassified | 20. NUMBER OF PAGES
91 | 21. PRICE
None |

Reproduction of completed page authorized

UCPRC ADDITIONAL INFORMATION

1.	DRAFT STAGE Final	2.	VERSION NUMBER 1
3.	PARTNERED PAVEMENT RESEARCH CENTER STRATEGIC PLAN ELEMENT NUMBER 4.64	4.	DRISI TASK NUMBER 3189
5.	CALTRANS TECHNICAL LEAD AND REVIEWER(S) Saeed Pourtahmasb	6.	FHWA NUMBER CA233189A

7. PROPOSALS FOR IMPLEMENTATION
No recommendations for implementation until the entire study is completed.

8. RELATED DOCUMENTS

9. LABORATORY ACCREDITATION
The UCPRC laboratory is accredited by AASHTO re:source for the tests listed in this report.

10. SIGNATURES

M. Elkashef **FIRST AUTHOR**	J.T. Harvey **TECHNICAL REVIEW**	C. Fink **EDITOR**	J.T. Harvey **PRINCIPAL INVESTIGATOR**	S. Pourtahmasb **CALTRANS TECH. LEADS**	T.J. Holland **CALTRANS CONTRACT MANAGER**

Reproduction of completed page authorized

DISCLAIMER

This document is disseminated in the interest of information exchange. The contents of this report reflect the views of the authors who are responsible for the facts and accuracy of the data presented herein. The contents do not necessarily reflect the official views or policies of the State of California or the Federal Highway Administration. This publication does not constitute a standard, specification, or regulation. This report does not constitute an endorsement by the Department of any product described herein.

For individuals with sensory disabilities, this document is available in alternate formats. For information, call (916) 654-8899, TTY 711, or write to California Department of Transportation, Division of Research, Innovation and System Information, MS-83, P.O. Box 942873, Sacramento, CA 94273-0001.

ACKNOWLEDGMENTS

PROJECT OBJECTIVES

This project is part of a larger study on asphalt mixes with high quantities of reclaimed asphalt pavement (RAP) and reclaimed asphalt shingles (RAS), Continued Development of Guidelines for Determining Binder Replacement in High RAP or RAS Mixes (PPRC Strategic Plan Element 4.64). The objective of this project is to develop guidelines for minimizing the risk of using high RAP and/or RAS contents in asphalt concrete mixes in California.

A major concern regarding evaluating high RAP or RAS mixes is the need to do extraction and recovery. The possibility to use mix testing to characterize high RAP or RAS mixes, to replace blending charts, will be assessed in this study. Mix testing should provide a means to evaluate cracking resistance and stiffness, and to rank mixes based on specified criteria. With the use of mix testing, extraction still needs to be done to determine the RAP binder content and the RAP gradation for volumetric mix design. The proposed mix testing should provide reliable and repeatable results. Otherwise, recommendations will be given to continue using blending charts to meet or exceed project specified binder performance grade.

This will be achieved in two phases, Phase 2 (Phase 1 was completed as part of Project Number 4.51a in the 2014-2017 contract).

Phase 2 tasks include the following:
- Task 1: Literature review of recently completed research.
- Task 2: Continued development and validation of testing procedures using fine aggregate matrix (FAM) mixes to determine the rheological properties of blended binders. Current Caltrans blending chart procedures, which require chemical extraction of the RAP/RAS binder, will be compared with FAM mix procedures. A suitable mix characterization test (e.g., semicircular bending [SCB] or indirect tensile asphalt cracking test [IDEAL-CT]) will also be identified for optimizing RAP/RAS contents in mixes.
- Task 3: Continued investigation into the blending mechanism and effectiveness of rejuvenating agents and the effect of the use of warm mix technologies and mix production at warm mix temperatures on binder replacement and long-term performance of mixes with high RAP or RAS binder replacement rates.
- Task 4: Continued investigation into understanding the aging rates and aging profiles of mixes containing high RAP or RAS contents and, if required, the refinement of laboratory procedures to simulate this aging. RAP variability across the state will be considered in this task.
- Task 5: Testing and evaluation of high RAP field mixes currently produced in California and recommendations about whether simple performance tests can be used for mix design approval or

blending charts should be used for high RAP mixes in Caltrans pilot projects in the summer of 2020. (This task was added to the scope in 2019.)

- Task 6: Preparation of a research report with interim recommendations for use of RAP and/or RAS as binder replacement and, if applicable, recommendations for accelerated pavement testing.

This report presents the initial results for Tasks 1 and 2 and completes Task 5.

EXECUTIVE SUMMARY

Short-term aging of asphalt mixes takes place during mixing, transportation, and placement. During production, asphalt plants can directly load mix into trucks for transport to the paving site or store mix in silos for a few to many hours before transporting it to the job site. Current standard specifications do not limit silo storage time. The ability to store mix in a silo is essential for maintaining a steady supply of hot mix to the paver during paving, considering available hours to mix, mixing plant and paving productivity rates, and breaks in paving caused by lane changes and equipment and trucking breakdowns.

The aging inside the silo is not accounted for during the mix design process, and it is not strictly accounted for in quality assurance procedures. In mixes that incorporate high amounts of reclaimed asphalt pavement/reclaimed asphalt shingles (RAP/RAS), additional blending can occur between the recycled and virgin binders while inside the silo. Moreover, high RAP or RAS mixes mostly include petroleum or bioderived additives called rejuvenators, depending on their chemical composition, to restore the properties of the mix. These rejuvenators may undergo physical or chemical changes during the silo storage, leading to further changes in the mix properties. Silo storage also increases aging of the virgin binder in the mix.

This study included a literature review and extensive performance-related testing to assess the effect of silo storage on the stiffness, rutting, cracking, and fatigue properties of high RAP or RAS mixes, including fine aggregate matrix mixes and full-graded mixes.

Key points from the literature review include the following:
- Addition of RAP/RAS increases mix stiffness and reduces fatigue cracking resistance at a given tensile strain level, which generally matches performance of the mix when used in thin overlays or new pavement layers. When used in thicker overlays and new pavement layers, the increased stiffness will decrease the tensile strain while also decreasing the fatigue life at a given tensile strain and the two counteracting influences need to be considered through mechanistic pavement structural analysis. Addition of RAP/RAS will reduce low-temperature and block cracking performance. Several mitigation measures can be taken to improve fatigue performance of mixes with RAP/RAS at a given strain and low-temperature and block cracking performance, including the use of softer virgin binders and rejuvenators.
- Blending between RAP/RAS and virgin binders is dependent on several factors, including mixing time and temperature as well the RAP/RAS stiffness and RAP/RAS content.
- A limited number of studies have investigated the effect of silo storage on the performance properties of asphalt mixes. The results indicate that the stiffness of the mixes increases with silo storage, and it was

generally concluded that additional blending takes place between the recycled and virgin binders inside the silo, increasing the effective binder content.

- The semicircular bending (SCB) test and indirect tensile asphalt cracking test (IDEAL-CT) are understood to provide a measure of the mix cracking resistance. Both tests were shown to provide good correlation with field performance—including thermal, reflective, and fatigue cracking—based on correlations with the performance of accelerated pavement test sections with 4.5 in. (110 mm) thick asphalt layers at the Federal Highway Administration (FHWA) accelerated loading facility and a number of other test sections.

- The flexural beam test has been historically validated to correlate with fatigue cracking in the field when the mix stiffness and fatigue life results are considered in a mechanistic pavement structural analysis.

Key observations from the flexural stiffness and rutting testing include the following:

- Mix A, with 50% RAP and a petroleum-based rejuvenator, and Mix B, with 40% RAP and a soft virgin binder, showed a lower modulus at higher temperatures compared with Mix C, with 20% RAP, 3% RAS, and a soft virgin, and Mix D, with 40% RAP and a small amount of biobased rejuvenator. This finding aligned with the Hamburg Wheel-Track (HWT) and repeated load triaxial (RLT) testing, which showed that Mix A and Mix B were more susceptible to rutting.

- The high rejuvenator dose used in Mix A resulted in a low modulus at high temperatures, leading to a reduction in the rutting resistance.

- The use of RAS in Mix C and the use of a low rejuvenator dose in Mix D resulted in a relatively high modulus at high temperatures and increased rutting resistance compared with the other mixes.

- The increase in modulus with silo storage was dependent on the test frequency and the mix design. The maximum increase in stiffness was about 50% to 60% and was noted at low test frequencies (i.e., high temperatures).

- Several parameters were successfully used to measure the rutting resistance of the mixes, including rut depth at 10,000 passes from the HWT, strain at 20,000 cycles from the confined RLT, and flow number and cycles at 5% strain from the unconfined RLT.

- Mix C, which included RAS, showed the best rutting performance while Mix A showed the lowest rutting resistance, possibly due to the use of a high rejuvenator dose.

- The rutting resistance of all the mixes was shown to increase with silo storage, except for the HWT test results for Mix D. The extent of change in rutting parameters varied between mixes and between rutting parameters.

Key observations from the SCB and IDEAL-CT testing include the following:

- The flexibility index (FI) from the SCB test and the cracking tensile index (CT$_{index}$) from the IDEAL-CT test showed strong correlation.

- The cracking resistance of the mixes decreased with silo storage as measured by the FI and CT_{index}.

- The cracking resistance of the mixes was inversely related to the rutting resistance. Mix C, with RAS, had the highest rutting resistance and lowest cracking resistance of all the mixes. On the other hand, Mix B, with 40% RAP and a rejuvenator, showed the lowest rutting resistance and highest cracking resistance of all the mixes.

- The FI was shown to correlate very well with the specimen vertical displacement, particularly the displacement given by the intercept of the post-peak slope. This indicates that the FI can be viewed as a direct measure of the specimen's ability to deform under load.

- The flexural stiffness at $20°C$ ($68°F$) and 10Hz (E50) showed good correlation with the IDEAL-CT strength, indicating that the IDEAL-CT test can be used to provide a measure of the mix stiffness.

- No correlation was found between the E50 parameter and the CT_{index}. The variability of the air voids of the FI specimens was high, as allowed under the version of the test when the specimens were prepared, which should be considered when interpreting these results. The variability of the air voids contents is not expected to change this conclusion.

Key observations from the flexural beam testing include the following:

- A strain-controlled flexural beam test showed that silo storage led to a reduction in the fatigue life of all mixes at high strain levels and mixed results at low strain levels.

- For all mixes, the strain at which a fatigue life of 250,000 cycles is reached decreased with silo storage.

- No correlation could be established between the cracking parameters—FI and CT_{index}—and the strain at a fatigue life of 250,000 cycles. The variability of the air voids of the FI specimens was high, which should be considered when interpreting these results. The variability of the air voids contents is not expected to change this conclusion.

Key observations from the fine aggregate matrix (FAM) mix testing include the following:

- Using linear amplitude sweep testing of FAM mixes, the fatigue life of FAM mixes was determined using the viscoelastic continuum damage model.

- The fatigue life of all FAM mixes decreased with silo storage. Similarly, the strain at which the fatigue life reached 250,000 cycles decreased with silo storage.

- The failure strain, defined as the peak phase angle, also decreased with silo storage for all FAM mixes.

- The failure strain from the FAM mix testing showed good correlation with the strain at 250,000 cycles from the flexural beam test.

- Using temperature-frequency sweep testing of FAM mixes, the modulus master curves of the FAM mixes showed similar ranking of the mixes compared with the modulus master curves of the full-graded mixes.

This indicates that FAM mix testing can be used to provide insight into the stiffness of the full-graded mixes.

The following conclusions are based on the summarized test results:

- The study revealed the significance of silo storage on mix properties. Based on the performance-related testing of full-graded and FAM mixes, silo storage has a notable effect on the properties of high RAP or RAS mixes and the effect is mix dependent. The results also showed that a notable change in mix properties can occur within the first few hours of silo storage (i.e., 5 to 6 hours).
- Cracking tests—the SCB and IDEAL-CT tests—are highly influenced by mix stiffness, which in turn is very sensitive to aging. The IDEAL-CT strength correlated very well with the flexural stiffness of the mix at 20°C (68°F) and 10Hz (E50). The variability of the air void contents of the SCB specimens was high.
- The FI from the SCB test and the CT_{index} from the IDEAL-CT test showed very good correlation. Both parameters appear to provide a good measure of the deformation ability of the mix under monotonic loading.
- The FI and CT_{index} did not directly correlate with four-point flexural beam (4PB) fatigue test results. Most notably, the FI and CT_{index} were not able to capture the poor fatigue performance of Mix A, with high rejuvenator dose and low binder content. Mix A had a low modulus at high temperatures due to the use of a high rejuvenator dose, and the low modulus resulted in a good FI and CT_{index} values. However, Mix A showed poor fatigue performance, possibly due to its low total and virgin binder contents.
- Proper selection of the rejuvenator dose is important to ensure satisfactory performance. Mix A, with a high rejuvenator dose, showed poor fatigue performance and exhibited rutting problems.
- Fatigue testing of FAM mixes showed promising results in terms of characterizing fatigue. However, at this stage, this testing is difficult to implement as a quality control/quality assurance test.
- Overall, the interactions of virgin binder grade, RAP content, rejuvenator dose, rejuvenator type, use of RAS, binder content, and silo storage are complex and cannot easily be explained due to conflicting effects and the likelihood of interactions. Performance-related testing provides a means to evaluate the net effects of these mix design and construction variables.

The following recommendations are made based on the findings from this study:

- The effect of silo storage on the performance properties of high RAP or RAS mixes should be taken into consideration when developing specifications for these types of mixes. The choice of sampling location can significantly change the performance-related testing results. If silo storage is expected to take place during actual production, the recommendation is that mixes be tested for performance-related properties

before and after silo storage as part of the job mix formula verification to better capture the range of expected values during production.

- The selection of the rejuvenator dose should not be based only on the manufacturer's recommendations. A systematic procedure that involves optimizing the dose based on performance should be adopted. One such procedure was recently introduced by the National Cooperative Highway Research Program Project 9-58. A maximum rejuvenator dose should not exceed 8% to 10% of total weight of the binder. The recommendation is also to consider the rejuvenator part of the recycled binder (i.e., the addition of a rejuvenator should not result in using less virgin binder).

- The SCB and IDEAL-CT tests can be used to provide a measure of the mix stiffness using the specimen strength.

- The results presented in this study suggest that the FI and CT_{index} should be used with caution as direct indicators of fatigue performance. Alternatively, the SCB and IDEAL-CT tests may be used to develop a criterion based on the relationship between stiffness and fatigue. Another UCPRC study looked at developing such fatigue criterion based on the testing of a wide range of mixes *(31)*.

- Inclusion of medium-term oven-aging procedure to capture some of the effects of the silo storage noted in this study, or in-place aging of the mix when not subjected to silo storage, should be included in future studies.

TABLE OF CONTENTS

LIST OF FIGURES

LIST OF TABLES

LIST OF ABBREVIATIONS

AASHTO	American Association of State Highway and Transportation Officials
COV	Coefficient of variance
DSR	Dynamic shear rheometer
FAM	Fine aggregate matrix
FHWA	Federal Highway Administration
FI	Flexibility index
HMA	Hot mix asphalt
HWT	Hamburg Wheel-Track
IDEAL-CT	Indirect tensile asphalt cracking test
I-FIT	Illinois Flexibility Index Test
JMF	Job mix formula
LAS	Linear amplitude sweep
NCHRP	National Cooperative Highway Research Program
PG	Performance grading
QC/QA	Quality control/quality assurance
PPRC	Partnered Pavement Research Center
RAP	Reclaimed asphalt pavement
RAS	Reclaimed asphalt shingles
RLT	Repeated load triaxial
SCB	Semicircular bending
SIP	Stripping inflection point
VECD	Viscoelastic continuum damage
4PB	Four-point flexural beam

LIST OF TEST METHODS AND SPECIFICATIONS USED IN THE REPORT

AASHTO M 320   Standard Specification for Performance-Graded Asphalt Binder

AASHTO M 323   Standard Specification for Superpave Volumetric Mix Design

AASHTO R 30   Standard Practice for Mixture Conditioning of Hot-Mix Asphalt (HMA)

AASHTO R 35   Standard Practice for Superpave Volumetric Design for Asphalt Mixtures

AASHTO TP 101   Estimating Damage Tolerance of Asphalt Binders Using the Linear Amplitude Sweep

AASHTO TP 124   Standard Method of Test for Determining the Fracture Potential of Asphalt Mixtures Using Semicircular Bend Geometry (SCB) at Intermediate Temperature

AASHTO T 84   Standard Method of Test for Specific Gravity and Absorption of Fine Aggregate

AASHTO T 85   Standard Method of Test for Specific Gravity and Absorption of Coarse Aggregate

AASHTO T 166   Standard Method of Test for Bulk Specific Gravity (Gmb) of Compacted Hot Mix Asphalt (HMA) Using Saturated Surface-Dry Specimens

AASHTO T 209   Standard Method of Test for Theoretical Maximum Specific Gravity (Gmm) and Density of Hot-Mix Asphalt

AASHTO T 312   Standard Method of Test for Preparing and Determining the Density of Asphalt Mix Specimens by Means of the Superpave Gyratory Compactor

AASHTO T 321   Standard Method of Test for Determining the Fatigue Life of Compacted Asphalt Mixtures Subjected to Repeated Flexural Bending

AASHTO T 331   Standard Method of Test for Bulk Specific Gravity (Gmb) and Density of Compacted Hot Mix Asphalt (HMA) Using Automatic Vacuum Sealing Method

SI* (MODERN METRIC) CONVERSION FACTORS

APPROXIMATE CONVERSIONS TO SI UNITS

Symbol	When You Know	Multiply By	To Find	Symbol
LENGTH				
in.	inches	25.40	millimeters	mm
ft.	feet	0.3048	meters	m
yd.	yards	0.9144	meters	m
mi.	miles	1.609	kilometers	km
AREA				
in^2	square inches	645.2	square millimeters	mm^2
ft^2	square feet	0.09290	square meters	m^2
yd^2	square yards	0.8361	square meters	m^2
ac.	Acres	0.4047	hectares	ha
mi^2	square miles	2.590	square kilometers	km^2
VOLUME				
fl. Oz.	fluid ounces	29.57	milliliters	mL
gal.	gallons	3.785	liters	L
ft^3	cubic feet	0.02832	cubic meters	m^3
yd^3	cubic yards	0.7646	cubic meters	m^3
MASS				
oz.	ounces	28.35	grams	g
lb.	pounds	0.4536	kilograms	kg
T	short tons (2000 pounds)	0.9072	metric tons	t
TEMPERATURE (exact degrees)				
°F	Fahrenheit	(F-32)/1.8	Celsius	°C
FORCE and PRESSURE or STRESS				
lbf	pound-force	4.448	newtons	N
lbf/in^2	pound-force per square inch	6.895	kilopascals	kPa

APPROXIMATE CONVERSIONS FROM SI UNITS

Symbol	When You Know	Multiply By	To Find	Symbol
LENGTH				
mm	millimeters	0.03937	inches	in.
m	meters	3.281	feet	ft.
m	meters	1.094	yards	yd.
km	kilometers	0.6214	miles	mi.
AREA				
mm^2	square millimeters	0.001550	square inches	in^2
m^2	square meters	10.76	square feet	ft^2
m^2	square meters	1.196	square yards	yd^2
ha	hectares	2.471	acres	ac.
Km^2	square kilometers	0.3861	square miles	mi^2
VOLUME				
mL	milliliters	0.03381	fluid ounces	fl. Oz.
L	liters	0.2642	gallons	gal.
m^3	cubic meters	35.31	cubic feet	ft^3
m^3	cubic meters	1.308	cubic yards	yd^3
MASS				
g	grams	0.03527	ounces	oz.
kg	kilograms	2.205	pounds	lb.
t	metric tons	1.102	short tons (2000 pounds)	T
TEMPERATURE (exact degrees)				
°C	Celsius	1.8C + 32	Fahrenheit	°F
FORCE and PRESSURE or STRESS				
N	newtons	0.2248	pound-force	lbf
kPa	kilopascals	0.1450	pound-force per square inch	lbf/in^2

*SI is the abbreviation for the International System of Units. Appropriate rounding should be made to comply with Section 4 of ASTM E380. (Revised April 2021)

1 INTRODUCTION

1.1 Background

Hot mix asphalt (HMA) containing reclaimed asphalt pavement (RAP) and/or reclaimed asphalt shingles (RAS) needs to be properly designed to perform well and to ensure that premature failure of the pavement does not occur. High RAP or RAS mixes typically exhibit high stiffness and, if used in surface layers, lead to problems with fatigue and thermal cracking. Current Caltrans specifications do not allow the use of RAS. The 2021 Revised Standard Specifications have the following requirements for use of RAP:

> For Type A HMA mixtures using RAP, the maximum allowed binder replacement is 25.0 percent in the upper 0.2 foot exclusive of OGFC [open friction grade course] and 40.0 percent below. The binder replacement is calculated as a percentage of the approved JMF [job mix formula] target asphalt binder content.
>
> For RAP substitution of 15 percent or less, the grade of the virgin binder must be the specified grade of asphalt binder for Type A HMA.
>
> For RAP substitution greater than 15 percent and not exceeding 25 percent, the grade of the virgin binder must be the specified grade of asphalt binder for Type A HMA with the upper and lower temperature classification reduced by 6 degrees C. Hamburg wheel track requirements are based on the grade of asphalt binder specified for Type A HMA.
>
> You may substitute RAP for part of the virgin aggregate in a quantity up to 25 percent of the aggregate blend.

RAP/RAS mixes with greater than 25% binder replacement are currently being used in California by local agencies and in commercial projects. Caltrans also has a non-Standard Special Provision (nSSP) for using up to 3% RAS by aggregate weight and up to 40% RAP by binder replacement.

Interest is growing among the asphalt pavement community in performance-related testing and specifications. The flexural beam test has historically been considered a reliable fatigue test, providing good correlation with field fatigue cracking. However, it is costly and time-consuming, which makes it very difficult to implement as a quality control/quality assurance (QC/QA) or routine mix design test. The semicircular bending (SCB) test, particularly the Illinois Flexibility Index Test (I-FIT) developed by the University of Illinois, and the indirect tensile asphalt cracking test (IDEAL-CT), developed by Texas A&M University, have been proposed as cracking tests to assess

various types of field cracking, including fatigue, thermal, and reflective cracking. As part of its efforts to investigate different performance-related tests, the California Department of Transportation (Caltrans) is interested in studying whether the SCB and IDEAL-CT tests can be used to identify mixes, particularly mixes containing RAP and/or RAS, with poor cracking and fatigue performance. In addition, the University of California Pavement Research Center (UCPRC) has been developing procedures for testing fine aggregate matrix (FAM) mixes as a possible QC/QA and routine mix design test—a simpler approach than the current flexural testing of full-scale mixes.

The Caltrans standard specifications do not state a limit for how long mixes can be held at high temperatures in a silo at an HMA plant before being hauled in trucks to the job site. Additional aging and blending are expected to take place inside the silo, affecting the mix properties. Silo storage times vary between projects and within the same project. These changes in mix properties, at different stages during production, make it challenging to draft specifications that assess the performance of the mixes, especially since this performance may vary greatly depending on the sampling location and silo storage duration.

Based on these issues, further investigation of the impact of silo storage duration on the properties of high RAP or RAS mixes is imperative. Also important is assessing the ability of the SCB and IDEAL-CT tests to flag high RAP or RAS mixes for poor fatigue cracking performance by comparing the results of those tests to results from the flexural beam test.

1.2   Problem Statements

During plant production, there is no limit on how long asphalt mixes can be stored in the silo before being transported to the construction site. Plant-produced mixes undergo additional aging during silo storage due to the high temperature in the silo, where aging of the virgin binder rather than of the RAP binder is the focus of the aging. This additional aging of the mixes is not accounted for during the mix design process and could greatly influence mix properties.

For mixes involving high RAP and/or RAS content, silo storage could also affect the mix properties by allowing additional blending between the RAP/RAS and virgin binders. Additional blending increases the amount of binder in the mix and increases the mix stiffness due to mobilization of a higher portion of the stiff RAP binder. Both factors contribute to the fatigue performance of the mix. Previous work at the UCPRC and by others in the laboratory has shown that additional blending takes place between the RAP/RAS and the virgin binders the longer the mix is kept at elevated temperatures, such as occurs during silo storage, until there is complete diffusion between them *(1)*. The blending of RAP binder and RAS binder from tear-off shingles (shingles that have been

taken off roofs after many years in service) are not expected to blend at the same rates and, potentially, the RAS binder may not blend at all because it is typically stiffer than RAP binder.

As a result of silo storage, additional recycled binder is activated and blends with the virgin binder, leading to an increase in available binder content. Moreover, the higher stiffness of the recycled binder compared with the virgin binder will lead to an overall increase in the binder's stiffness as more recycled binder becomes available. As noted, greater aging reduces the fatigue life of a mix at a given tensile strain, while increasing the available binder content increases the fatigue life at a given strain. The overall impact of silo storage on high RAP or RAS mixes becomes even more complex because most of these mixes use rejuvenators to restore the properties of the recycled binder and promote blending. These rejuvenators may undergo certain physiochemical changes during silo storage, leading to yet another change in mix properties.

For the reasons previously discussed, the study of the effects of silo storage on mix properties, particularly for high RAP or RAS mixes, is of paramount importance. Because current Caltrans standard specifications effectively limit the use of RAP to a maximum of 25% by weight of dry aggregate, mixes included in this study were selected from local agencies or commercial projects that were not designed according to Caltrans specifications. Caltrans also has an nSSP for using up to 3% RAS by aggregate weight and up to 40% RAP by binder replacement that is primarily being used on pilot projects.

1.3   Study Objectives

This study is part of UCPRC Project 4.64. The part of the project included in this report involves testing and evaluation of high RAP field mixes currently produced in California to develop recommendations about whether simple performance tests should be implemented to replace blending charts for mix design approval for high RAP mixes in Caltrans pilot projects during the summer of 2020 (projects that were postponed due to the COVID pandemic). The objectives of this study are the following:

- Provide a literature review of the topics related to this study.
- Provide a preliminary evaluation of the ability of simple mix tests, such as the SCB and IDEAL-CT tests, to flag high RAP or RAS mixes based on comparison of parameters from the simple tests with the performance-related properties of flexural beam fatigue and stiffness.
- Further investigate the use of FAM testing to evaluate fatigue cracking performance in the laboratory.
- Investigate the effects of silo time on the blending, aging, and resultant change in properties of high RAP or RAS mixes.

To achieve these objectives, plant-produced mixes were collected from different regions within California, before and after silo storage. The plant-produced mixes were sampled at the hot drop point directly from the plant discharge as well as from the silo after storage for several hours.

1.4   Report Layout

This research report is organized as follows:

- Chapter 2 provides a literature overview of the topics related to this study.
- Chapter 3 summarizes the sampling and testing plan for the four plant-produced mixes that were included in this study.
- Chapter 4 presents the results of the flexural stiffness and modulus master curves from the temperature-frequency sweep flexural testing. The rutting performance results are also summarized and discussed in relation to the stiffness properties, and the impact of silo storage on rutting is assessed.
- Chapter 5 presents the cracking test results from the SCB and IDEAL-CT tests. The overall cracking resistance of the mixes is analyzed, and the impact of silo storage on cracking is assessed.
- Chapter 6 presents the results of the flexural beam testing and investigates the relationship between the cracking tests and the fatigue testing.
- Chapter 7 summarizes the FAM mix test results, including the fatigue and stiffness of the FAM mixes.
- Chapter 8 provides a project summary, conclusions, and preliminary recommendations.

2 LITERATURE REVIEW

2.1 High RAP or RAS Mixes

The use of recycled materials, such as RAP and RAS, in HMA to replace more expensive virgin asphalt binder and aggregate is becoming more common. An important motivation for the use of increased amounts of RAP and RAS in HMA is a reduction in cost. Estimates of cost reductions for use of RAP/RAS compared with mixes that only have virgin binder are shown in Table 2.1. Rough calculations show how these cost savings occur. If the approximate cost of a ton of virgin asphalt binder is $600 per ton and it is 5% of the total mass of the mix and the approximate cost of the virgin aggregate in the mix is $40, then the rough material costs are $68 per ton of asphalt concrete (0.05*$600+0.95*$40). If the approximate cost of RAP with a 5% binder content is $40 per ton and 20% RAP by mass is used in the mix and 20% RAP binder replacement is assumed, then the approximate material cost is $62.40 per ton (0.04*$600+0.95*0.8*$40+0.2*$40), an 8% savings. If the RAP is free, then the 20% RAP mix material cost is $54.4 per ton, a 20% cost savings. Milling, transportation, storage, and processing of RAP have costs not included in this rough calculation, However, milling and transportation costs are typically a bid item in the contract that produces the RAP, leaving primarily the storage and processing costs. The costs of rejuvenating or recycling agents would need to be included for mixes with greater amounts of RAP. These cost calculations can be adjusted as the price of virgin binder, virgin aggregate, and RAP change, but they show how the cost savings shown in Table 2.1 can occur.

Table 2.1: Potential Cost Savings with RAP and RAS[a]

Material	Cost Savings
5% RAS[b]	2%-5%[b]
20% RAP[c]	>16%[c]
50% RAP[c]	>40%[c]
25% RAP[d]	14%-20%[d]
50% RAP[d]	29%-35%[d]

[a] Source: Newcomb, Epps, and Zhou (2)
[b] Source: Zhou et al. (3)
[c] Source: Brock (4)
[d] Source: Willis et al. (5)

Specifications regulating the use of RAP and RAS can be developed to ensure that the performance of these mixes is within acceptable limits. If not designed properly, mixes containing RAP or RAS could exhibit premature failure due to the increased stiffness caused by inclusion of the recycled binder and result in the early appearance of cracking distresses, including fatigue and thermal cracking (6,7), which would negate cost savings from the use in construction. The use of a softer virgin binder in the Caltrans standard specifications, for mixes containing more than 25% RAP by weight of dry aggregate and up to 25% RAP, is meant to compensate for the expected increase in the mix stiffness. If the virgin binder in the mix is required to have reduced stiffness through binder grade

reduction, the risk of early rutting of the mix exists if the RAP binder does not mobilize and blend with the virgin binder.

To allow for more RAP to be incorporated into asphalt mixes, numerous research studies have investigated the effect of high RAP content on the mix performance *(8,9)*. High RAP is generally defined as RAP content exceeding 25% of the total content of the mix by mass, or RAP binder exceeding 25% of the total binder content by mass. More precisely, the RAP content can be measured as the percentage of RAP by weight of dry aggregate or the percentage of RAP binder content in the total binder content. The percentage of RAP by weight of dry aggregate is easier to calculate since it does not involve RAP binder extraction to determine the RAP binder content. However, the percentage of RAP by weight of dry aggregate does not account for the effect of RAP binder content on the mix properties. This effect is very important because the impact of RAP on the mix properties is largely determined by the percentage of RAP binder replacing the virgin binder, and different RAP stockpiles can have significantly different binder contents, in addition to different aging characteristics. The impact of the RAP binder replacement becomes more significant when dealing with mixes containing high RAP, particularly when the RAP is highly aged.

Introducing mixes with high RAP content poses many challenges related to the mix design and selection of additives, quality control, mix production and placement, and field performance. Several performance-related properties have been identified as significant when assessing high RAP mixes, including stiffness, resistance to permanent deformation, fatigue, and fracture-related properties. The addition of RAP tends to increase the stiffness of the mix and reduce both its thermal cracking resistance and fatigue cracking resistance at a given tensile strain level *(2,3,10)*. Fatigue cracking reductions are critical for surface mixes and thin overlays. The balancing of stiffness and mix fatigue resistance at a given strain level achieves optimal structural fatigue resistance that uses thicker layers of asphalt, with stiffer mixes generally providing better structural fatigue life as long as the fatigue resistance of the mix at a given strain level is not severely reduced *(11)*. Different alternatives have been proposed to reduce or eliminate the impact of RAP, including using a softer virgin binder or adding a rejuvenator *(12,13)*.

2.2 Silo Storage

Current design guidelines for mixes containing high RAP use blending charts that assume a state of full blending between the RAP and virgin binders *(5,14)*. However, achieving full blending is dependent on several factors, including RAP stiffness and content, mixing temperature and time, and binder layer thickness *(15,16)*. Blending between the recycled binder and virgin binder may continue to take place when the mix is stored at an elevated temperature inside a silo at the plant prior to transport to the construction site and laydown. One study showed

that the impact of silo storage is more significant for mixtures containing RAP than for virgin mixes, with the increase in the mix stiffness as high as 80% for a silo storage time of 10 hours *(17)*. Another study suggested that prolonged silo storage, in addition to promoting blending, leads to aging of the asphalt mix even in an inert atmosphere *(18)*. The effect of silo storage on both the thermal cracking resistance and fatigue behavior of RAP mixes was also studied by collecting plant samples for different silo storage times *(19,20)*. The thermal cracking resistance improved with silo storage as shown by a decrease in the fracture temperature. Moreover, the results of the flexural beam fatigue testing showed improve fatigue life with silo storage.

2.3   Performance-Related Tests

Cracking is a primary distress of asphalt pavements that can generally be divided into four main categories: (1) thermal, (2) bottom-up fatigue, (3) top-down fatigue, (4) and reflective cracking *(21)*. Recently, there has been widely growing interest in performance-related testing to characterize different aspects of mix performance. National Cooperative Highway Research Program (NCHRP) Project 9-57 identified several desirable features for a cracking test, including simplicity, repeatability, and correlation to field performance *(21)*. A version of the SCB test developed by the University of Illinois, the I-FIT test, is conducted at an intermediate temperature using a monotonic loading *(22)*. A flexibility index is calculated from the I-FIT test and used to assess the cracking resistance of the mixes.

The indirect tensile asphalt cracking test developed by Texas A&M, the IDEAL-CT test, is essentially an indirect tensile test conducted at an intermediate temperature, and it is a simple and practical alternative to the SCB test *(23)*. Both the I-FIT and IDEAL-CT tests appear to correlate well with field performance in terms of fatigue, thermal, and reflective cracking in the studies reviewed *(23,24,25)*. The IDEAL-CT test showed good correlation with measurements of field cracking at the Federal Highway Administration (FHWA) accelerated loading facility conducted in 2013 in sections with approximately 4.5 in. (112 mm) thick asphalt *(23)*. The same accelerated pavement test sections from the FHWA Turner-Fairbanks aerated loading facility were used to validate the SCB I-FIT test *(25)*. A limited number of field test sections in Texas were also used to validate the IDEAL-CT test *(23)*. A recent study conducted by the National Center for Asphalt Technology using seven different mixes showed that both the SCB and IDEAL-CT tests were able to discriminate between cracked and uncracked test sections using short-term oven-aging conditioned lab mix-lab compacted specimens *(24)*.

The flexural beam fatigue test has been validated over years of work to correlate with field fatigue cracking when used in pavement analysis also considering stiffness, and it is used to provide mix fatigue characterization for the *CalME* design software used by Caltrans. The Strategic Highway Research Program Project A-003A developed a testing and analysis procedure using four-point flexural fatigue *(26)*. Fatigue failure in pavements is induced by

repetitive loading leading to a gradual deterioration in the material properties (damage). The SCB and IDEAL-CT tests apply monotonic loading at a constant rate and thus do not simulate traffic-induced fatigue loading.

2.4   Literature Review Summary

Key points from the literature review relevant to this study include the following:

- The addition of RAP/RAS increases mix stiffness, reduces thermal cracking resistance, and reduces fatigue cracking resistance at a given strain level. Several mitigation measures can be taken to improve performance of mixes with RAP/RAS, including the use of softer virgin binders and rejuvenators.

- Blending between RAP/RAS and virgin binders is dependent on several factors, including mixing time and temperature as well the RAP/RAS stiffness and content.

- A limited number of studies have investigated the effect of silo storage on the performance properties of asphalt mixes. The results indicated that the stiffness of the mixes increases with silo storage and that additional blending takes place between the recycled and virgin binders inside the silo.

- The I-FIT and IDEAL-CT tests are believed to provide a measure of the mix cracking resistance. Both tests were shown to correlate well with field performance—including thermal, reflective, and fatigue cracking—based on correlations with the performance of accelerated pavement test sections from the FHWA accelerated loading facility in relatively thin 4.5 in. thick (112 mm) asphalt sections and several other test sections.

- The flexural beam test has been validated by years of work to correlate with fatigue cracking in the field and has provided inputs for mechanistic-empirical design software.

3   SAMPLING AND TESTING PLAN OF ASPHALT MIXES

The focus of this study is HMA mixes containing high RAP and RAS. As noted previously, HMA mixes designed according to Caltrans specifications did not fit the requirements of this study and hence were not considered. The mixes included in this study were selected from mixes currently produced for local agencies and commercial projects across California. Because of time limitations and mix availability, every effort was taken to select mixes that represent a wide range of materials and additives from across California. The UCPRC worked with several asphalt producers to identify four plant-produced mixes. The plant-produced mixes were sampled under two different aging conditions: (1) a hot drop directly from the plant discharge and (2) after hours of silo storage. Samples were collected on the day of mix production using a sampling trailer with a one-ton capacity hopper and a quartering device. Mixes were collected in five-gallon metal buckets. The buckets were reheated to a temperature of 135°C (275°F) in the lab to split the mixes into test size samples. Prior to compaction, the samples were heated at the compaction temperature of 135°C (275°F) for 90 minutes.

3.1   Plant-Produced Mixes

The mixes selected for this study are shown in Table 3.1.

Table 3.1: Plant-Produced Mixes Used in the Study

Mix ID	Silo Storage Time (hrs)	Total Asphalt Content (% by mass of mix)	Recycled Material (% of total mass of aggregate)	Rejuvenator (% of virgin binder by mass)	Virgin Binder (PG)	Mixing Temperature [(ºC) (ºF)]
Mix A-0H	0	5.1	50% RAP	20% petroleum-based	PG 64-10	145 (293)
Mix A-6H	6					
Mix B-0H	0	5.9	40% RAP	n/a	PG 58-28	160 (311)
Mix B-16H	16					
Mix C-0H	0	5.2	20% RAP/ 3% RAS	n/a	PG 58-22	145 (293)
Mix C-5H	5					
Mix D-0H	0	5.8	40% RAP	0.7% vegetable oil-based	PG 64-10	155 (302)
Mix D-16H	16					

In the absence of any previous comprehensive studies on the impact of silo storage, it was difficult to decide on an appropriate range of silo storage times. In addition, the selection of the silo storage time for each mix was largely controlled by the asphalt mix plant to ensure that the sampling work did not disrupt plant operations. Accordingly, a wide range of silo storage times, between 5 and 16 hours, was included in the study, shown in Table 3.1.

Two of the mixes, Mix A and Mix D, contained a rejuvenator and a PG 64-10 virgin binder. Mix A contained a high dose of an aromatic extract petroleum-based rejuvenator, while Mix D contained a low dose of a biobased rejuvenator. The selected doses were based on the manufacturer's recommendations and were calculated as a percentage of the virgin binder. The other two mixes, Mix B and Mix C, did not contain a rejuvenator but used a soft virgin binder with PG 58-28 and PG 58-22, respectively. More information regarding the mixes is shown in Table 3.1, including total binder content and mixing temperature. The performance grades of the RAP or RAS binders were not available. Information about the RAP or RAS binder contents were only available for some mixes. Detailed descriptions of each of the four mixes are included in the following sections.

3.1.1 Mix A (50% RAP + Rejuvenator)

Mix A was sampled from an asphalt plant in Los Angeles County. The mix design was done according to the Marshall method, where specimens are compacted using a mechanical hammer with 75 blows on each side according to the procedure outlined in the Asphalt Institute's *MS-2 Asphalt Mix Design Methods* manual. The RAP gradation and total aggregate gradation of the mix are shown in Figure 3.1. The mix contained 50% RAP by weight of dry aggregate. An aromatic extract petroleum-based rejuvenator was added to the mix at 20% by weight of virgin binder. The rejuvenator was introduced to the mix through blending with the virgin binder before mixing with aggregate and RAP.
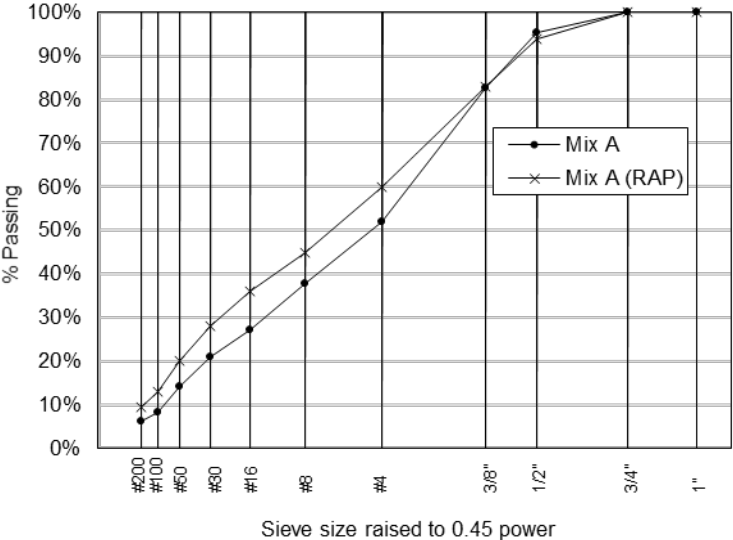
Note: The mix code is %RAP-%RAS-%rejuvenating agent. RAP and RAS percentages are by mass of mix; rejuvenating agent percentage is by mass of total binder. Example: 50RAP-20RJ is 50% RAP, no RAS, and 20% rejuvenating agent.

Figure 3.1: Total and RAP aggregate gradation for Mix A (50RAP-20RJ).

3.1.2   Mix B (40% RAP + Soft Virgin Binder)

Mix B was sampled from an asphalt plant in Fresno County. This mix had a nominal maximum aggregate size of ½", and it is typically used to pave commercial parking lots. The mix contained 40% RAP by weight of dry aggregate, and a soft PG 58-28 binder was used in lieu of a rejuvenator in this environment that has hot summer temperatures. The RAP aggregate gradation and total aggregate gradation are shown in Figure 3.2.

Note: The mix code is %RAP-%RAS-%rejuvenating agent. RAP and RAS percentages are by mass of mix; rejuvenating agent percentage is by mass of total binder. Example: 50RAP-20RJ is 50% RAP, no RAS, and 20% rejuvenating agent.

Figure 3.2: Total and RAP aggregate gradations for Mix B (40RAP).

3.1.3   Mix C (20% RAP + 3% RAS + Soft Virgin Binder)

Mix C was sampled from an asphalt plant in Sacramento County. The mix had a nominal maximum aggregate size of ½" and it was designed according to the Superpave method. It contained 20% RAP and 3% RAS by weight of dry aggregate. The RAP binder content was 4.1% by total weight of RAP, and the RAS binder content was 22.4% by total weight of RAS. A soft PG 58-22 binder was used, and no rejuvenator was added to the mix. The RAP aggregate gradation and total aggregate gradation are shown in Figure 3.3.
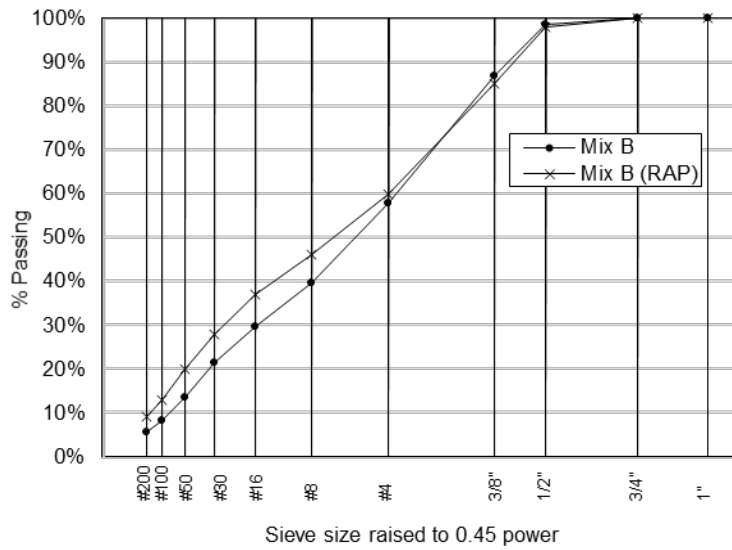
Note: The mix code is %RAP-%RAS-%rejuvenating agent. RAP and RAS percentages are by mass of mix; rejuvenating agent percentage is by mass of total binder. Example: 50RAP-20RJ is 50% RAP, no RAS, and 20% rejuvenating agent.

Figure 3.3: Total, RAP, and RAS aggregate gradations for Mix C (20RAP-3RAS).

3.1.4   Mix D (40% RAP + Rejuvenator)

Mix D was sampled from an asphalt plant in Ventura County. The mix has a nominal maximum aggregate size of ½" and it was designed according to the Superpave method. The mix had 40% RAP by weight of dry aggregate, and the RAP binder content was 4.95% by total weight of RAP. A vegetable oil-based rejuvenator was used at a dose of 0.7% by weight of virgin binder. The RAP aggregate gradation and total aggregate gradation are shown in Figure 3.4.
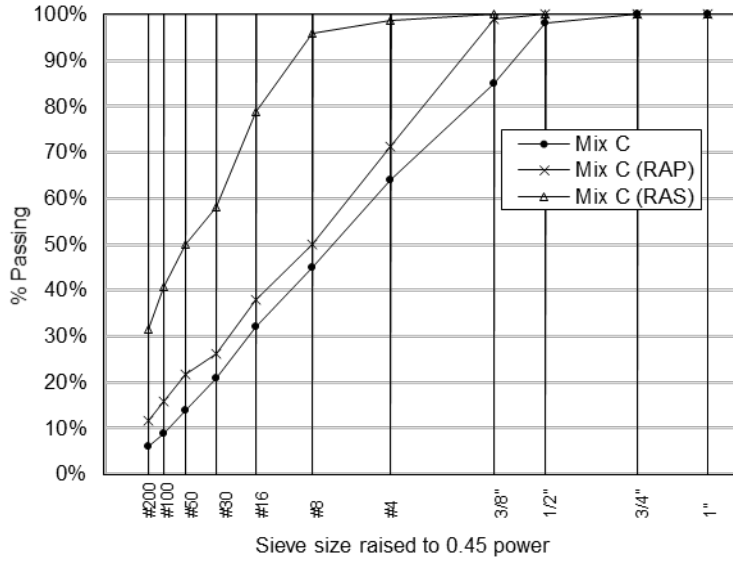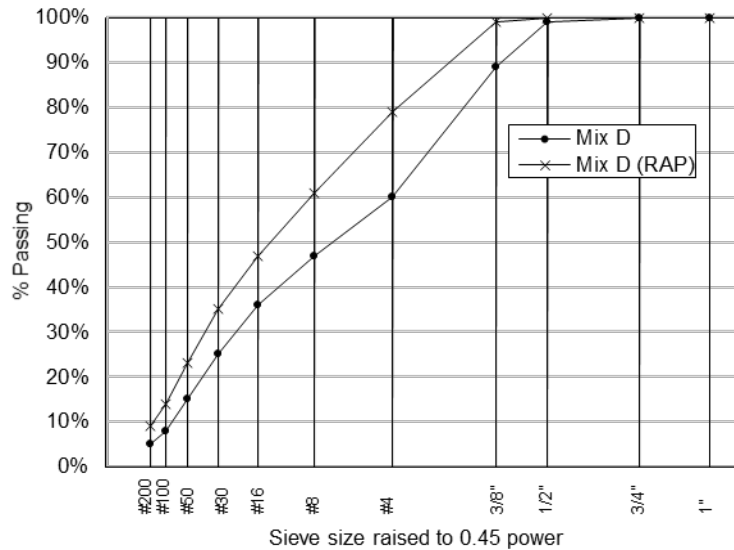
Note: The mix code is %RAP-%RAS-%rejuvenating agent. RAP and RAS percentages are by mass of mix; rejuvenating agent percentage is by mass of total binder. Example: 50RAP-20RJ is 50% RAP, no RAS, and 20% rejuvenating agent.

Figure 3.4 : Total and RAP aggregate gradations for Mix D (40RAP-0.7RJ).

3.2   Performance-Related Testing

The mixes were compacted and tested in the laboratory to characterize different properties, including stiffness, rutting, cracking, and fatigue. To assess rutting performance, Hamburg Wheel-Track (HWT) and repeated load triaxial (RLT) tests using both confined and unconfined configurations were used. The HWT test is currently specified by Caltrans for measuring rutting and moisture susceptibility of asphalt mixes. The RLT test was introduced as part of the NCHRP Project 9-19 study to determine the permanent deformation characteristics of asphalt mixes. The tertiary flow in the asphalt mix can be defined by the flow number indicating the number of load cycles at the onset of the tertiary flow. A confining pressure can be applied during the RLT test to better simulate the confinement conditions of the asphalt mix inside the pavement.

The cracking performance in terms of fracture was assessed using both the SCB and IDEAL-CT tests. Both tests provide a measure of the cracking resistance of asphalt mixes under a constant monotonic loading rate. The cracking resistance is evaluated using the flexibility index (FI) from the SCB test and the cracking tensile index (CT_{index}) from IDEAL-CT. The higher the FI and CT_{index} values, the better the cracking resistance. Fatigue performance was characterized using the flexural fatigue test, and mix stiffness master curves were developed using flexural frequency sweep tests.

3.2.1   Rutting

The plant-produced mixes were compacted in the lab using a Superpave gyratory compactor and tested for rutting using the HWT and RLT tests according to AASHTO T 324 and AASHTO T 378, respectively. In accordance with the Caltrans standard specifications, the HWT test was conducted at a temperature of 50°C (122°F) using Superpave gyratory compacted samples measuring 60±1 mm in height. For each mix, four specimens were compacted to run two HWT tests. HWT tests were run up to a maximum of 35,000 passes, and HWT samples were compacted to a target air void of 7±1%. The average, maximum, and minimum air void contents of all the tested samples are shown in Figure 3.5.
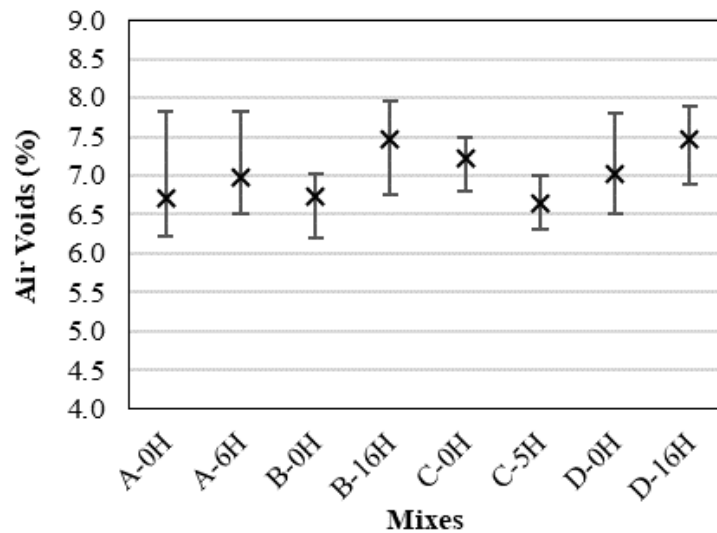
Figure 3.5: Air void contents for the HWT test specimens.

The RLT test was conducted according to AASHTO T 378, procedure B, using both confined and unconfined conditions at a test temperature of 45°C (113°F). For each test, a minimum of three samples was compacted and tested. Specimens were compacted using a Superpave gyratory compactor according to AASHTO R 83. A minimum of two samples were used to calculate an average permanent deformation. For the confined RLT tests, a confining pressure of 35 KPa and a deviator stress of 483 KPa were applied. To run the unconfined RLT test, a deviator stress of 483 KPa was applied. The tests were terminated at a maximum of 20,000 cycles or a maximum permanent axial strain of 5%. The air void contents of the specimens prepared for RLT testing are shown in Figure 3.6 and Figure 3.7, for the unconfined and confined test configurations, respectively.
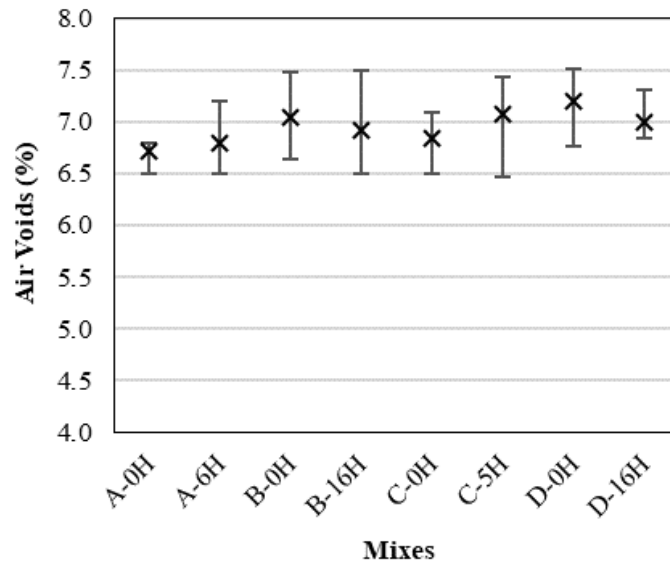
Figure 3.6: Air void contents for the unconfined RLT test specimens.
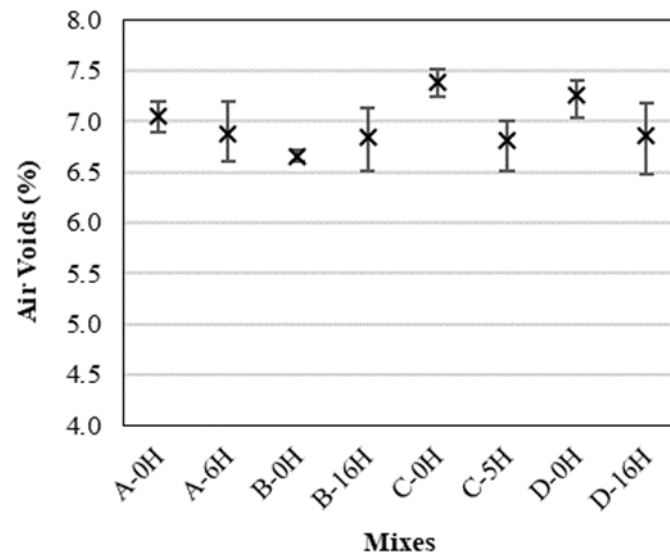
Figure 3.7: Air void contents for the confined RLT test specimens.

3.2.2   Cracking (Fracture)

SCB I-FIT Test

Semicircular bending (SCB) tests were performed following AASHTO TP 124-18 at a temperature of 25°C (77°F). To prepare the SCB specimens, the gyratory compacted specimens were trimmed to provide smooth faces and then cut into two discs. The target air void content of the discs was 7±1% based on the 2018 version of the test used when the specimens were prepared in 2019. The discs were then cut into two halves providing two semicircular specimens. The test was run using notched semicircular specimens, and the flexibility index (FI)

parameter was calculated from the load-deformation curve. The air void content of the tested SCB specimens is shown in Figure 3.8, with the error bars representing the range of air voids. The range of air void contents is high for the test specimens, which introduces more variability into the results.
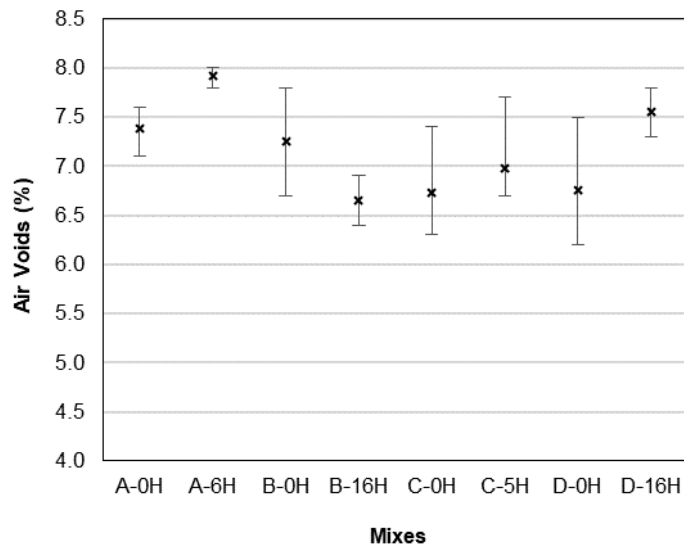
Figure 3.8: Air void contents for the SCB test specimens.

IDEAL-CT Test

IDEAL-CT tests were performed per ASTM D8225-19. Specimens were compacted using a Superpave gyratory compactor with a diameter of 150 mm and a height of 62 mm at a target air void of 7±0.5%. The compacted specimens were tested directly without the need for trimming, cutting, or notching. The test was conducted at a temperature of 25°C (77°F). The average air void content of the IDEAL-CT specimens for different mixes is shown in Figure 3.9. The error bars indicate the maximum and minimum air void content.
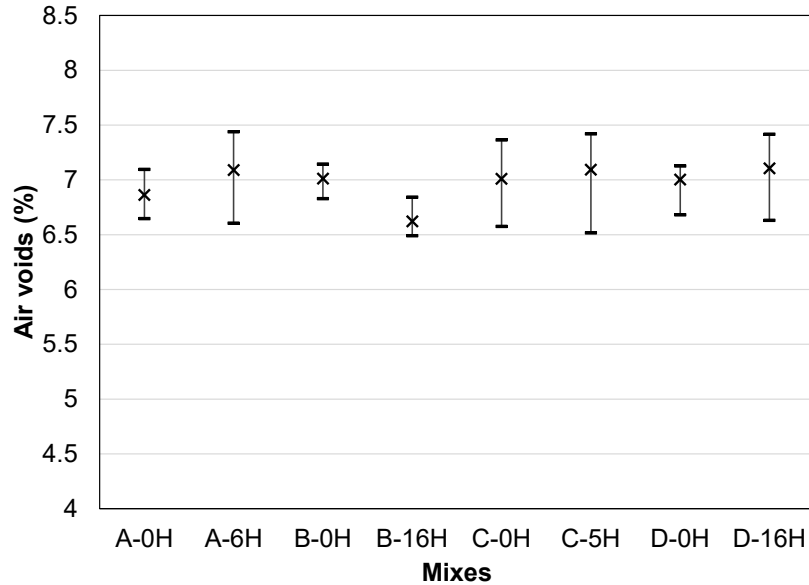
Figure 3.9: Air void contents of IDEAL-CT specimens.

3.2.3   Flexural Beam Fatigue and Stiffness

To assess the fatigue performance of the mixes, flexural beam fatigue testing using strain-controlled loading was conducted according to AASHTO T 321. The test was conducted at a temperature of 20°C (68°F) and a frequency of 10 Hz using three different strain levels. The strain levels were different for each mix and intended to produce fatigue lives of approximately 0.05, 0.5, and 1 million repetitions to failure. At each strain level, three specimens were tested for a total of nine tested specimens per mix. Specimens were prepared according to AASHTO PP3 using a rolling wheel compactor.

Flexural beam temperature-frequency sweep tests were also conducted according to AASTHO T 321. For each mix, three specimens were tested. Temperature-frequency sweep testing was conducted at three different temperatures (10°C [50°F], 20°C [68°F], 30°C [86°F]) and 11 frequencies (0.01 Hz, 0.02 Hz, 0.05 Hz, 0.1 Hz, 0.2 Hz, 0.5 Hz, 1.0 Hz, 2.0 Hz, 5.0 Hz, 10.0 Hz, 15.0 Hz) using a strain level of 0.0001. Figure 3.10 shows the air void contents and air void range for the tested flexural beam specimens.

Figure 3.10: Air void contents of flexural beam specimens.

4 STIFFNESS AND RUTTING BEHAVIOR

4.1 Stiffness Master Curves

The temperature-frequency sweep test results were used to construct stiffness master curves for the plant-produced mixes, collected before silo storage, as shown in Figure 4.1. The stiffness master curves were obta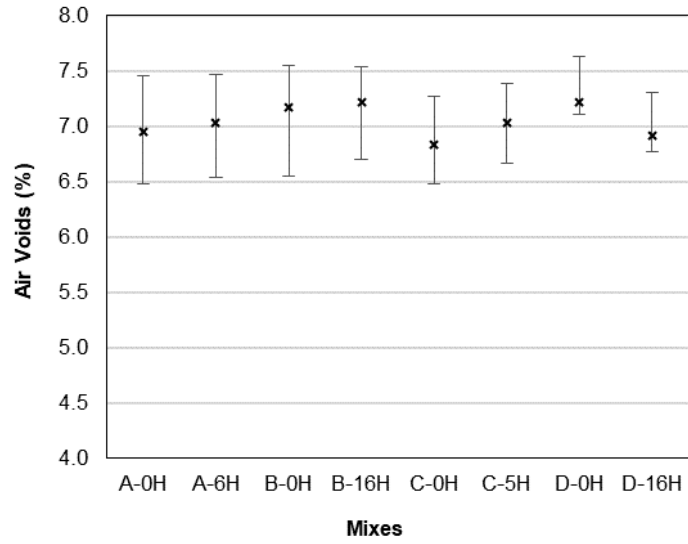ined at a reference temperature of 20°C (68°F). Mix A and Mix B showed lower modulus values, particularly at lower frequencies (i.e., higher temperatures), compared with Mix C and Mix D. Mix A is interesting because it is softer than Mix C and Mix D at lower reduced frequencies (lower frequencies and higher temperatures) and stiffer than those mixes at higher reduced frequencies. The reason why this occurred is not known.
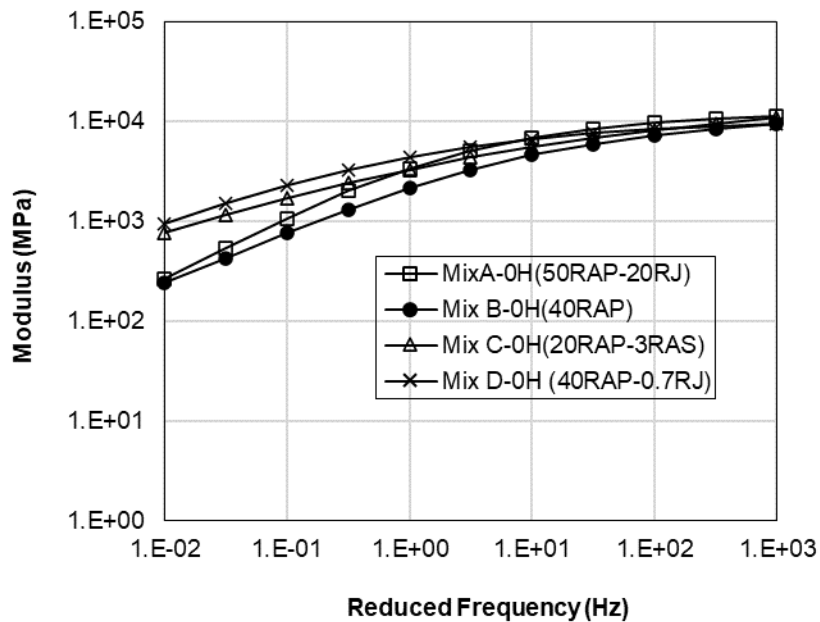
Note: The mix code is %RAP-%RAS-%rejuvenating agent. RAP and RAS percentages are by mass of mix; rejuvenating agent percentage is by mass of total binder. Example: 50RAP-20RJ is 50% RAP, no RAS, and 20% rejuvenating agent.

Figure 4.1: Flexural modulus master curves for mixes with no silo storage at a reference temperature of 20°C (68°F).

To quantify the effect of silo storage on the different mixes, the ratio of the modulus after silo storage to the modulus before silo storage was calculated, shown in Figure 4.2. The relative increase in modulus due to silo storage was found to be dependent on the test frequency and to vary between the different mixes and their associated different silo storage times. A ratio of as high as 1.5 to 1.6—an increase of 50% to 60% in the modulus—was noted after silo storage.

Mix A had a shorter amount of silo aging than Mix B and Mix D (6 hours versus 16 hours), but it had more stiffening at lower frequencies. In addition, it should be noted that Mix C had less aging than Mix B and Mix D (5 hours versus 16 hours), but it had more stiffening than Mix B and similar stiffening to Mix D.

Overall, these results indicate that the complex interactions of the different variables—base binder, RAP content, RAS content, rejuvenator type and content, and silo storage time—produce net results that are not easy to predict based on the expected individual effects of each variable.

Notes:
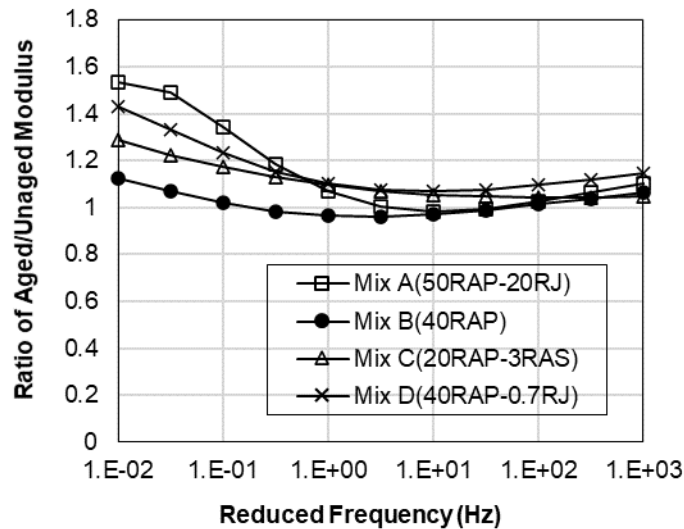 - Silo storage times are A: 6 hours, B: 16 hours, C: 5 hours, D: 16 hours.
  - The mix code is %RAP-%RAS-%rejuvenating agent. RAP and RAS percentages are by mass of mix; rejuvenating agent percentage is by mass of total binder. Example: 50RAP-20RJ is 50% RAP, no RAS and 20% rejuvenating agent.

Figure 4.2: Effect of silo storage on the modulus master curves for all mixes.

4.2   Initial Flexural Stiffness at 20ºC and 10 Hz from Fatigue Tests

The initial flexural stiffness of the mixes during flexural fatigue tests was determined at a temperature of 20ºC (68ºF) and a frequency of 10 Hz. The stiffness measurements during the first few cycles of loading were influenced by the self-heating of the mix during loading and are therefore not considered in the analysis. To exclude the effect of self-heating and to capture the stiffness prior to any fatigue damage, the flexural stiffness was measured at 50 loading cycles. Fatigue testing was performed at three different strain levels, and the initial stiffness at 50 cycles (E50), shown in Figure 4.3 represents an average stiffness across all three different strain levels.

The results in Figure 4.3 clearly indicate that the initial stiffnesses of the mixes increased with silo storage. Mix A appears to have a higher stiffness compared with the other mixes at the reference temperature and frequency. However, the modulus master curve of Mix A (Figure 4.1) shows that the stiffness of Mix A decreased at higher temperatures compared with the other mixes, particularly Mix C and Mix D. The modulus master curves provided in Figure 4.1 can be used to estimate the flexural stiffness at the different loading conditions, and the modulus master curves shown in Figure 4.1 show that the ranking of the mixes based on their modulus depends on the loading frequency (i.e., test temperature). Ranking of the mixes according to their stiffnesses based on Figure 4.3 would only be applicable at the given temperature and frequency and should not be assumed to be valid for other test temperatures and loading frequencies.
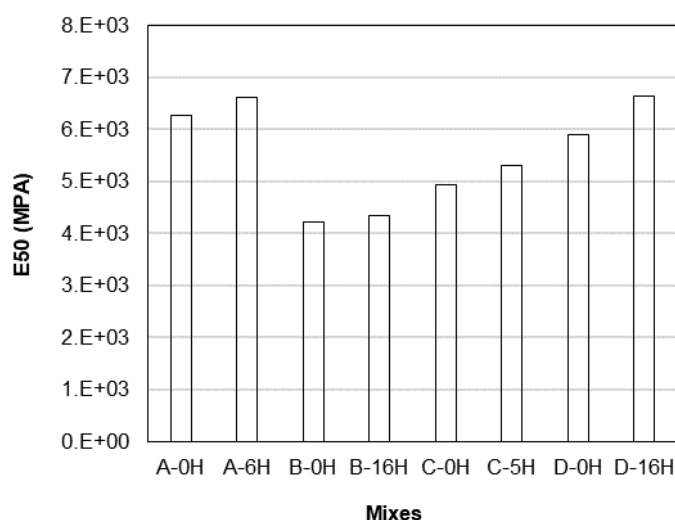
Note: Identification of mixes is mix-hours of silo time.

Figure 4.3: Flexural stiffness at 20ºC (68ºF) and 10Hz (E50) for all mixes with and without silo storage.

4.3   Rutting Test Results

4.3.1   Hamburg Wheel-Track Test

The Hamburg Wheel-Track (HWT) test was conducted for all mixes to assess their rutting and moisture sensitivity performance. Table 4.1 shows the variability for the HWT test for each mix and silo condition.

Table 4.1: Coefficient of Variation of HWT Rut Depth at 25,000 Passes for Mixes and Silo Conditions

Mixes	A-0H	A-6H	B-0H	B-16H	C-0H	C-5H	D-0H	D-16H
Coefficient of Variation (COV) (%)	67.4	15.4	4.8	7.1	3.3	2.9	3.8	13.1

Note: Rut depth in millimeters (mm).

Figure 4.4 to Figure 4.7 show the change in rut depth with the number of passes for all four mixes before and after silo storage. The results clearly show that the rutting resistance of the mixes improved after silo storage, as evidenced by the decrease in the average rut depths, except for Mix D, which showed a small decrease in rutting resistance. The relative increase in rutting resistance due to silo storage was not consistent across all mixes due to the differences in the composition of the mixes and in the silo storage time. Of the mixes, Mix A showed the most notable improvement in rutting resistance because of silo storage (Figure 4.4). Mix A uses a high rejuvenator dose, which resulted in low mix stiffness and low rutting resistance with no silo storage time. The rutting resistance of Mix A significantly increased after 6 hours of silo storage.
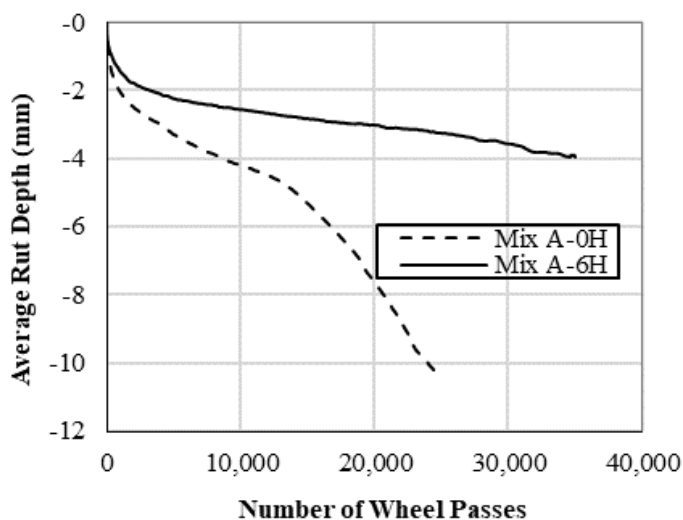
Note: The mix code is %RAP-%RAS-%rejuvenating agent. RAP and RAS percentages are by mass of mix; rejuvenating agent percentage is by mass of total binder. Example: 50RAP-20RJ is 50% RAP, no RAS, and 20% rejuvenating agent.

Figure 4.4: Average rut depth versus number of wheel passes from HWT test of Mix A (50RAP-20RJ).
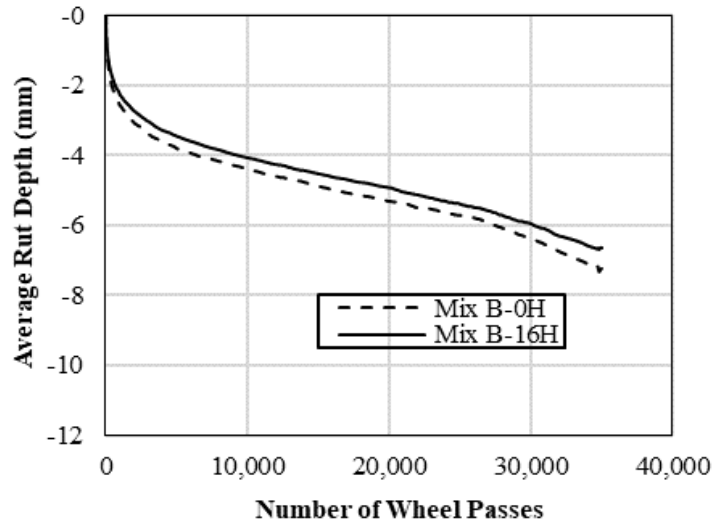
Note: The mix code is %RAP-%RAS-%rejuvenating agent. RAP and RAS percentages are by mass of mix; rejuvenating agent percentage is by mass of total binder. Example: 50RAP-20RJ is 50% RAP, no RAS, and 20% rejuvenating agent.

Figure 4.5: Average rut depth versus number of wheel passes from HWT test of Mix B (40RAP).

Note: The mix code is %RAP-%RAS-%rejuvenating agent. RAP and RAS percentages are by mass of mix; rejuvenating agent percentage is by mass of total binder. Example: 50RAP-20RJ is 50% RAP, no RAS, and 20% rejuvenating agent.

Figure 4.6: Average rut depth versus number of wheel passes from HWT test of Mix C (20RAP-3RAS).
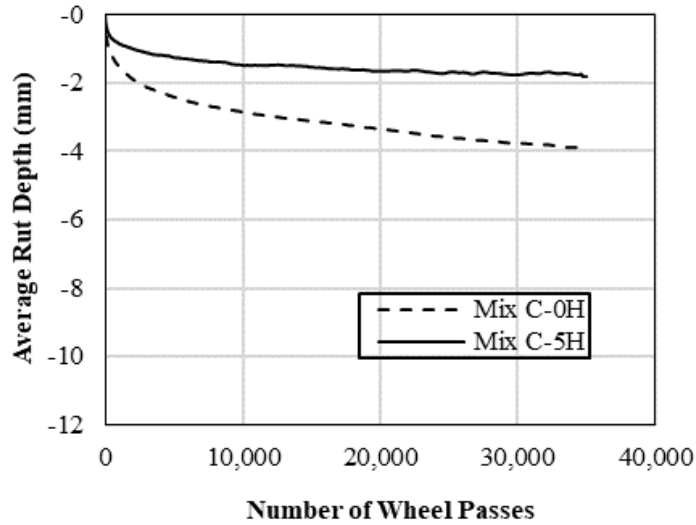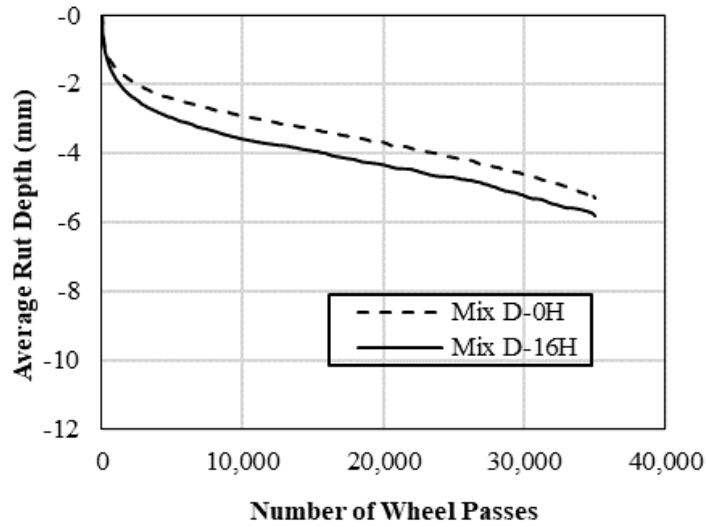
Note: The mix code is %RAP-%RAS-%rejuvenating agent. RAP and RAS percentages are by mass of mix; rejuvenating agent percentage is by mass of total binder. Example: 50RAP-20RJ is 50% RAP, no RAS, and 20% rejuvenating agent.

Figure 4.7: Average rut depth versus number of wheel passes from HWT test of Mix D (40RAP-0.7RJ).

To quantify the effect of the silo storage on rut depth, the average rut depth was calculated at 10,000, 20,000, and 25,000 passes, shown in Figure 4.8.
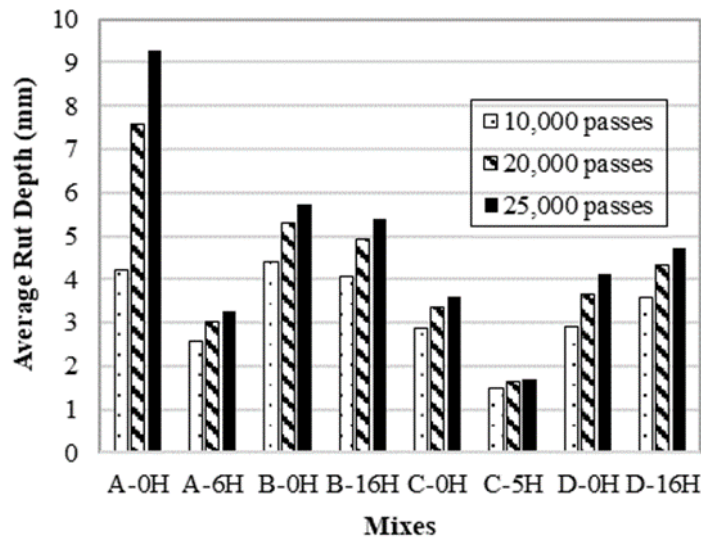
Figure 4.8: Average rut depth from HWT test for all mixes.

The stripping inflection point (SIP) from the HWT test was calculated for all mixes and plotted in Figure 4.9. Mix A and Mix B showed a SIP indicating the potential for stripping due to moisture. The silo-aged material for

Mix A did not show the same strong inflection point. On the other hand, no SIP was noted for Mix C and Mix D, indicating no susceptibility to moisture damage. The Caltrans standard specifications do not specify a passing criterion for the SIP but do require it to be reported.
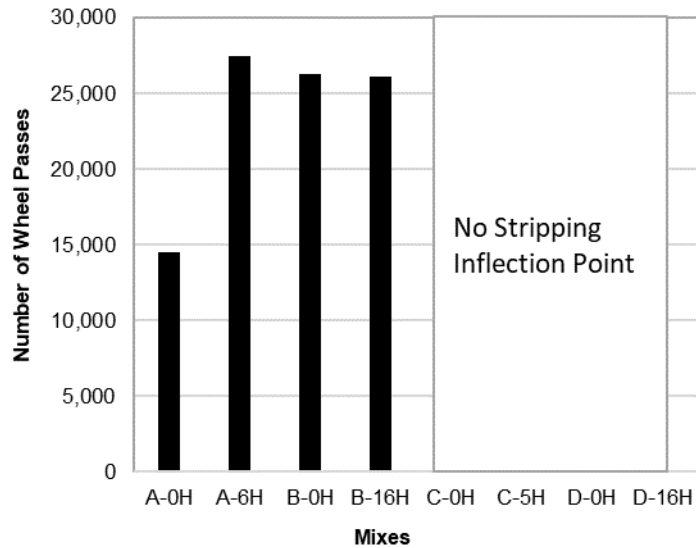
Figure 4.9: Average number of wheel passes at the stripping inflection point.

### 4.3.2 Repeated Load Triaxial Test

The results of the confined repeated load triaxial (RLT) test, before and after silo storage, are shown in Figure 4.10 to Figure 4.13. The variability of the unconfined RLT cycles to 5% permanent strain are shown in Table 4.2.

Table 4.2: Coefficient of Variation of Unconfined RLT Cycles to 5% Permanent Strain for Mixes and Silo Conditions

Mixes	A-0H	A-6H	B-0H	B-16H	C-0H	C-5H	D-0H	D-16H
Coefficient of Variation (COV) (%)	24.0	28.1	55.0	30.2	20.5	Not applicable[a]	17.4	18.5

[a] None of the Mix C specimens reached 5% permanent strain after five hours of silo time; test was stopped at 20,000 cycles.

For all mixes, the permanent axial strain at a given load cycle decreased after silo storage. A decrease in the permanent axial strain denotes an improvement in the rutting resistance. The accumulated permanent strain curves for the confined RLT test show a primary and a secondary zone. The primary zone is characterized by a rapid increase in the axial strain, indicating initial consolidation of the mix, followed by a secondary zone where the rate of increase in permanent strain appears to reach a steady state. For the confined RLT test, a tertiary zone,

indicating internal cracking leading to rapid deformation, was not noted for any of the tested mixes before or after silo storage.

On the other hand, the results of the unconfined RLT test, shown in Figure 4.14 to Figure 4.17, clearly indicate the occurrence of tertiary flow in all mixes. The permanent axial strains measured in the unconfined RLT test were much higher than those measured in the confined RLT test due to the absence of confining pressure. However, it is, clear that both the confined and unconfined tests were able to capture the effect of silo storage on the average permeant strain. For the confined RLT test results, the effects of silo storage are particularly strong for Mix A, which only had 6 hours of silo time but had 20% rejuvenator, and for Mix D, which had 16 hours of silo time. For the unconfined RLT test results, Mix C and Mix D showed the greatest effects of silo storage time.
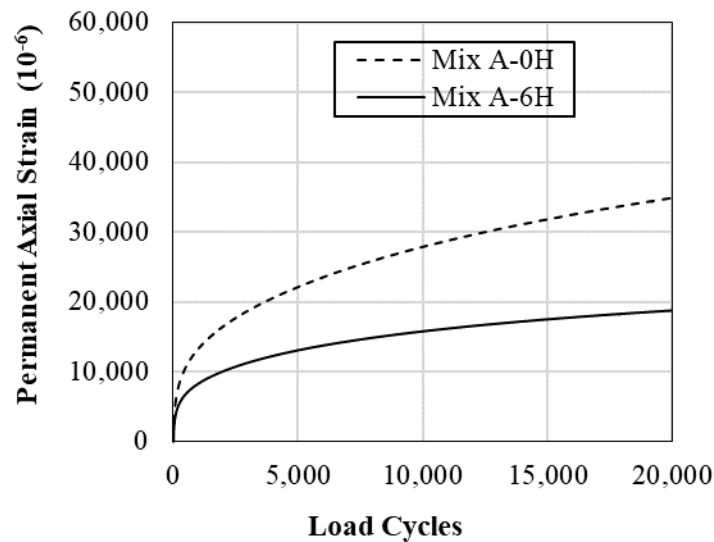
Note: The mix code is %RAP-%RAS-%rejuvenating agent. RAP and RAS percentages are by mass of mix; rejuvenating agent percentage is by mass of total binder. Example: 50RAP-20RJ is 50% RAP, no RAS, and 20% rejuvenating agent.

Figure 4.10: Permanent axial strain versus load cycles for confined RLT tests of Mix A (50RAP-20RJ).
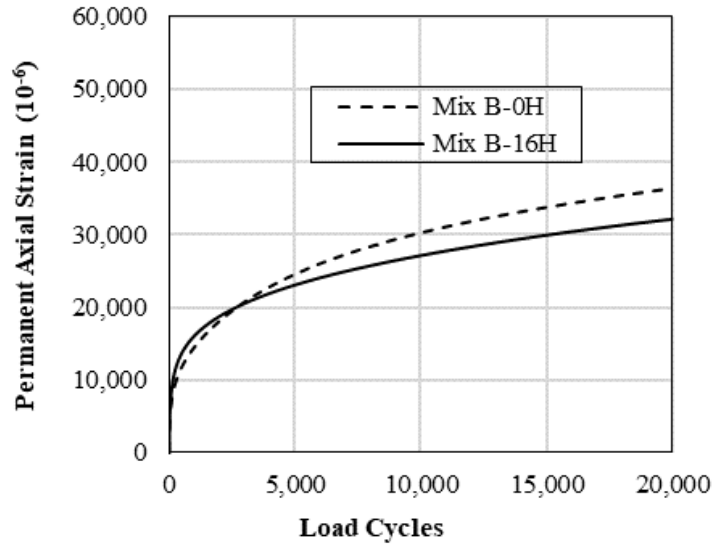
Note: The mix code is %RAP-%RAS-%rejuvenating agent. RAP and RAS percentages are by mass of mix; rejuvenating agent percentage is by mass of total binder. Example: 50RAP-20RJ is 50% RAP, no RAS, and 20% rejuvenating agent.

Figure 4.11: Permanent axial strain versus load cycles for confined RLT tests of Mix B (40RAP).

Note: The mix code is %RAP-%RAS-%rejuvenating agent. RAP and RAS percentages are by mass of mix; rejuvenating agent percentage is by mass of total binder. Example: 50RAP-20RJ is 50% RAP, no RAS, and 20% rejuvenating agent.

Figure 4.12: Permanent axial strain versus load cycles for confined RLT tests of Mix C (20RAP-3RAS).

Note: The mix code is %RAP-%RAS-%rejuvenating agent. RAP and RAS percentages are by mass of mix; rejuvenating agent percentage is by mass of total binder. Example: 50RAP-20RJ is 50% RAP, no RAS, and 20% rejuvenating agent.

Figure 4.13: Permanent axial strain versus load cycles for confined RLT tests of Mix D (40RAP-0.7RJ).

Note: The mix code is %RAP-%RAS-%rejuvenating agent. RAP and RAS percentages are by mass of mix; rejuvenating agent percentage is by mass of total binder. Example: 50RAP-20RJ is 50% RAP, no RAS, and 20% rejuvenating agent.

Figure 4.14 : Permanent axial strain versus load cycles for unconfined RLT tests of Mix A (50RAP-20RJ).

Note: The mix code is %RAP-%RAS-%rejuvenating agent. RAP and RAS percentages are by mass of mix; rejuvenating agent percentage is by mass of total binder. Example: 50RAP-20RJ is 50% RAP, no RAS, and 20% rejuvenating agent.

Figure 4.15: Permanent axial strain versus load cycles for unconfined RLT tests of Mix B (40RAP).
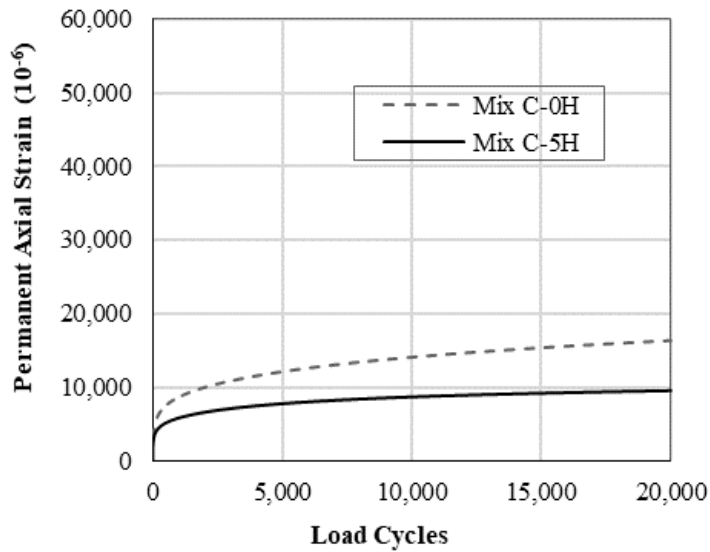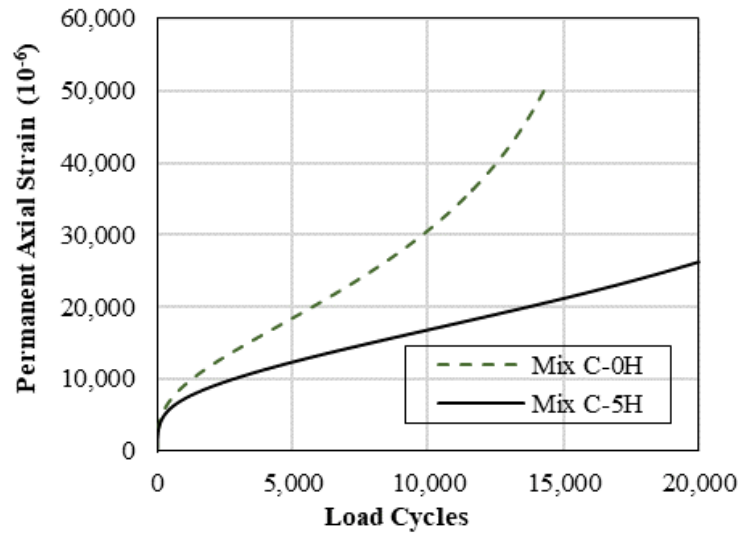

Note: The mix code is %RAP-%RAS-%rejuvenating agent. RAP and RAS percentages are by mass of mix; rejuvenating agent percentage is by mass of total binder. Example: 50RAP-20RJ is 50% RAP, no RAS, and 20% rejuvenating agent.

Figure 4.16: Permanent axial strain versus load cycles for unconfined RLT tests of Mix C (20RAP-3RAS).
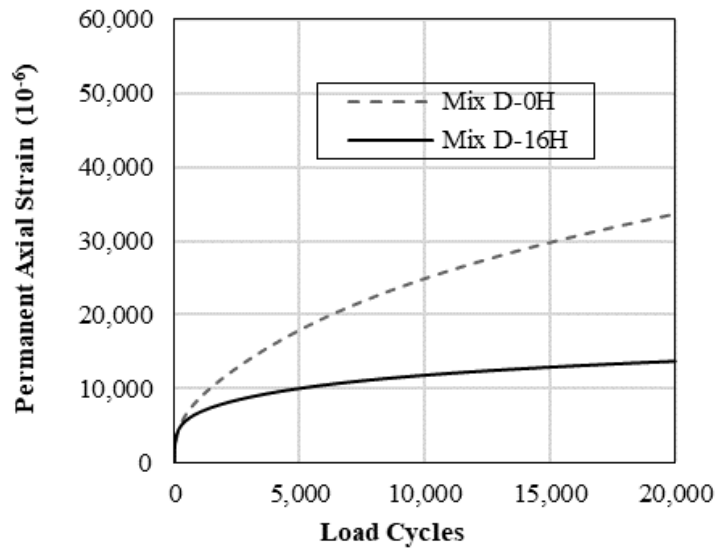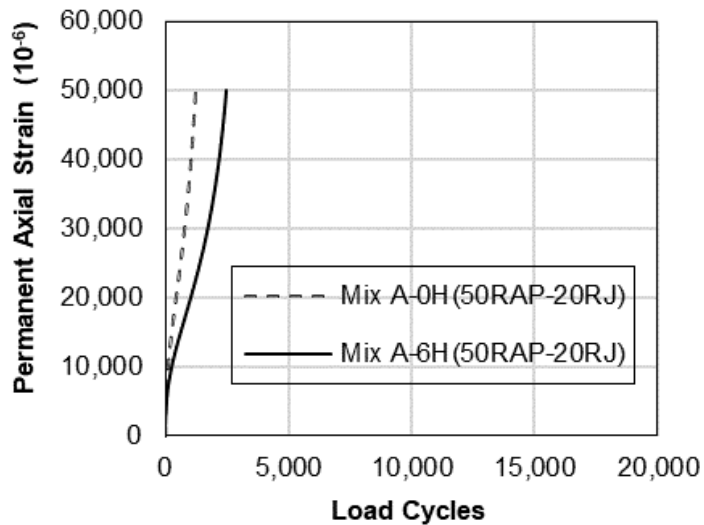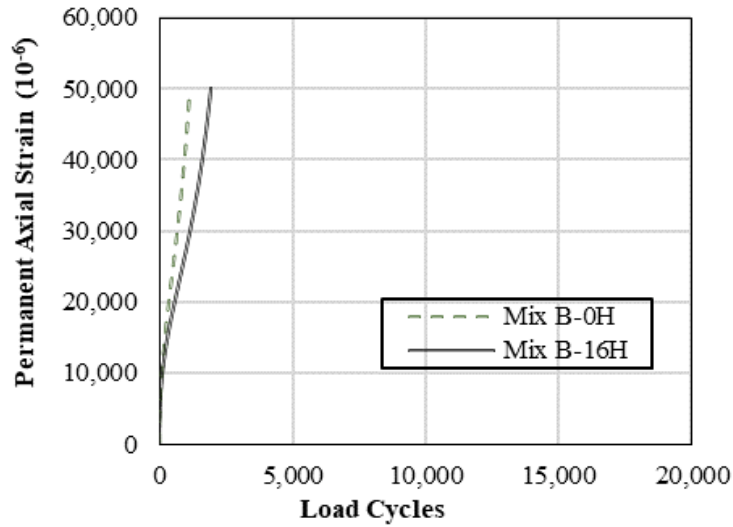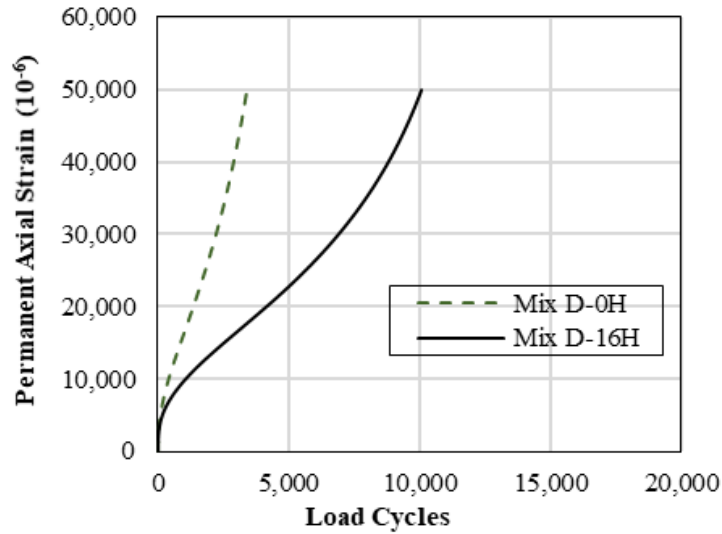
Note: The mix code is %RAP-%RAS-%rejuvenating agent. RAP and RAS percentages are by mass of mix; rejuvenating agent percentage is by mass of total binder. Example: 50RAP-20RJ is 50% RAP, no RAS, and 20% rejuvenating agent.

Figure 4.17: Permanent axial strain versus load cycles for unconfined RLT tests of Mix D (40RAP-0.7RJ).

Using the RLT unconfined test results, the number of loading cycles at 5% permanent axial strain was calculated and plotted, shown in Figure 4.18 for all mixes. This parameter serves as an indication of the mix resistance to axial permanent deformation. A higher number of loading cycles indicates an improved resistance to axial deformation and thus less susceptibility to rutting. The rutting resistance, as measured by the average number of loading cycles at 5% strain, was noted to increase with silo storage. Mix C-0H had high rutting resistance and for Mix C-5H, the permanent strain did not reach 5% at the end of testing (i.e., 20,000 loading cycles).
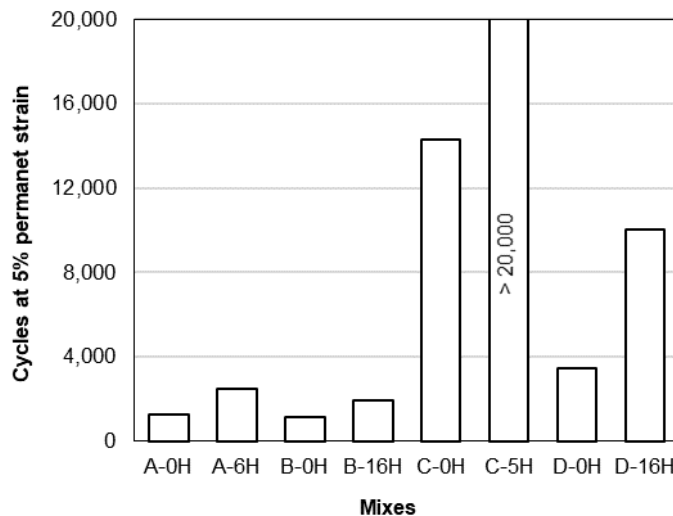
Figure 4.18: Cycles at 5% permanent strain from unconfined RLT test.

The flow number, representing the number of cycles at the start of the tertiary zone, is commonly used to analyze the RLT test results. Figure 4.19 shows the flow number plotted against the number of loading cycles at 5% permanent axial strain. The results clearly indicate a very good correlation between the two parameters—flow number and the number of loading cycles at 5% permanent strain. The calculation of the flow number depends on the accuracy of the model used to fit the accumulated permanent strain curve. On the other hand, the number of loading cycles at 5% permanent strain can be directly obtained from the test results, which makes it easier to use as a QC/QA parameter.
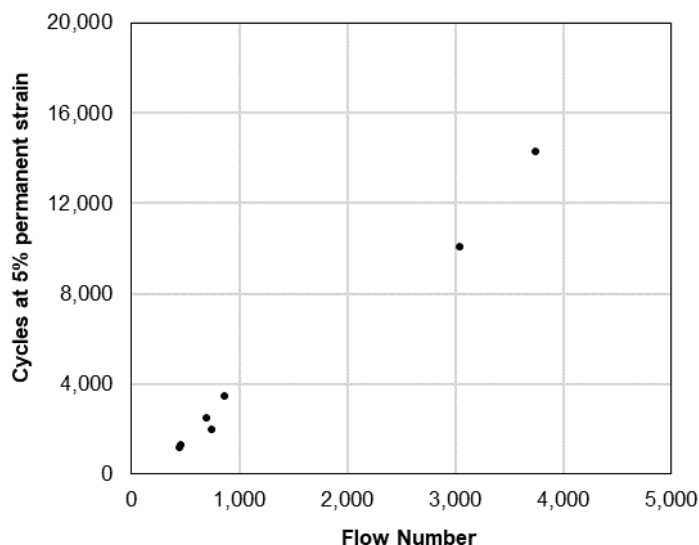
Figure 4.19: Correlation between flow number and number of cycles at 5% permanent strain from unconfined RLT test.

4.4   Analysis of Rutting Parameters

To further assess the effect of silo storage time on rutting, a statistical analysis using a t-test was conducted to compare the rutting performance of the mixes before and after silo storage. The t-test was based on the rut depth at 10,000 passes from the HWT and the cycles to 5% permanent strain from the unconfined RLT. The p-values, expressed as a percentage, are provided in Table 4.3. The decrease in rut depth was statistically significant for all the mixes for both tests, based on a 90% confidence limit.

Table 4.3: P-Values for the Rutting Parameters Sensitivity to Silo Storage

Mixes	P-Value (HWTT rut depth at 10,000 passes) [%]	P-Value (cycles to 5% permanent strain) [%]
Mix A (50RAP-20RJ)	3.6	0.6
Mix B (40RAP)	7.6	3.7
Mix C (20RAP-3RAS)	0.4	not applicable*
Mix D (40RAP-0.7RJ)	9.0	0.0

* None of the Mix C specimens reached 5% permanent strain after 5 hours of silo time, test was stopped at 20,000 cycles.

Note: The mix code is %RAP-%RAS-%rejuvenating agent. RAP and RAS percentages are by mass of mix; rejuvenating agent percentage is by mass of total binder. Example: 50RAP-20RJ is 50% RAP, no RAS, and 20% rejuvenating agent.

To compare results of the unconfined RLT test and the HWT test for the materials subjected to zero hours and hours of silo storage, the cycle at 5% strain was plotted against the rut depth at 10,000 passes, shown in Figure 4.20. For Mix C, at five hours of silo storage time, the cycle at 5% strain was assumed to be 20,000. Generally, mixes exhibiting a high HWT rut depth showed a low number of cycles at 5% strain, whereas mixes with a low rut depth showed a high number of cycles at 5% strain.
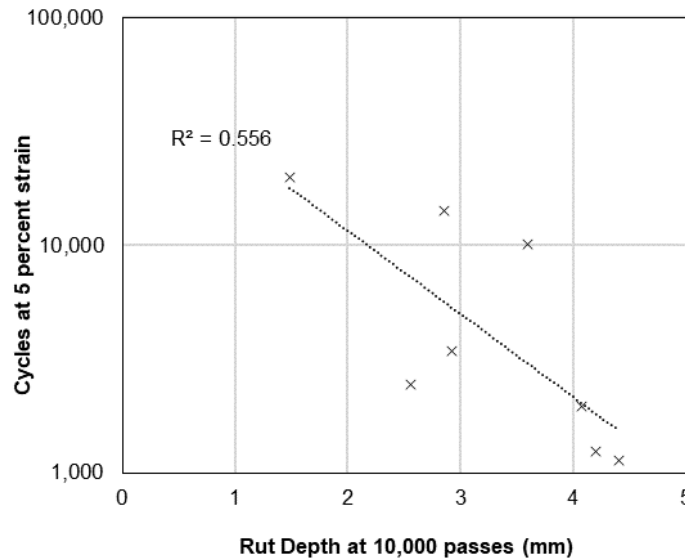
Figure 4.20: Correlation between rut depth from HWT test and cycles at 5% strain from unconfined RLT for both silo storage conditions.

The rut depth at 10,000 passes was also plotted against the flow number, shown in Figure 4.21. Generally, mixes with high rut depths showed low flow numbers whereas mixes with low rut depth showed high flow numbers. It should be noted that none of the HWT test results showed a rut depth greater than 5 mm.
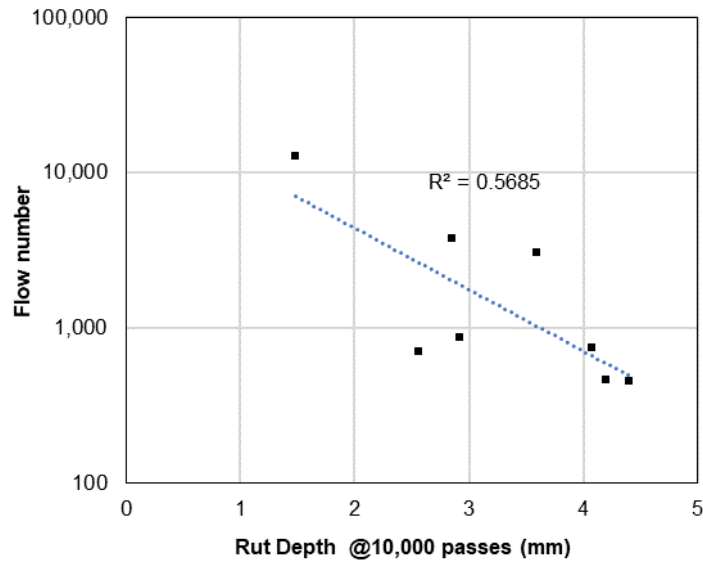
Figure 4.21: Correlation between rut depth from HWT test and flow number from unconfined RLT for both silo storage conditions.

The flow number and the cycles at 5% strain are used to indicate performance based on the unconfined RLT test data. However, they cannot be used in conjunction with the confined RLT test since the test does not typically result in tertiary flow or high permanent strain levels. To analyze the confined RLT test results, the permanent axial strain at 20,000 loading cycles was determined for all mixes, and the correlation between the permanent axial strain and other rutting parameters was calculated. A good correlation was noted between the strain at 20,000 cycles and the HWT test rut depth at 10,000 passes, shown in Figure 4.22. The strain at 20,000 cycles from the confined RLT test correlated very well with the flow number from the unconfined RLT test, shown in Figure 4.23.
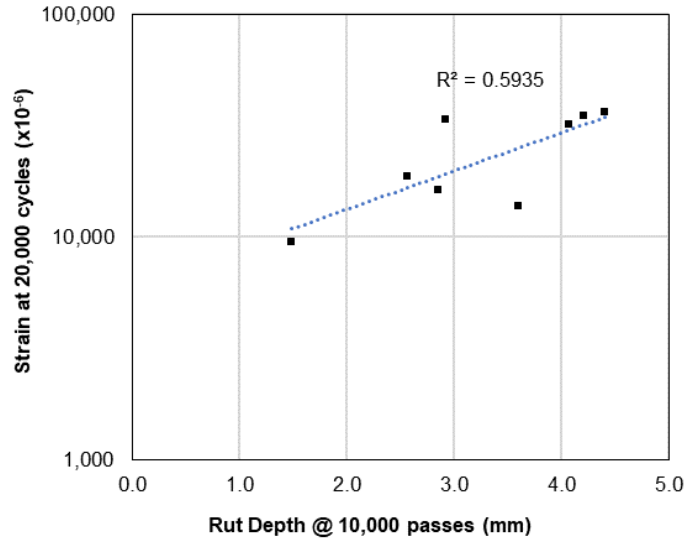
Figure 4.22: Correlation between rut depth from HWT test and permanent strain at 20,000 passes from confined RLT for both silo storage conditions.
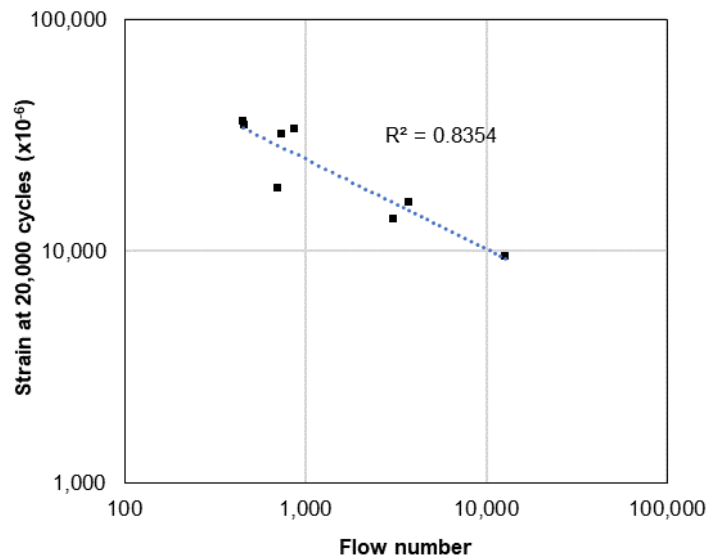
Figure 4.23: Correlation between flow number from unconfined RLT test and permanent strain at 20,000 cycles from confined RLT test for both silo storage conditions.

4.5   Effect of Silo Storage on Rutting Parameters

The different correlations between the rutting parameters, presented in the previous section, indicate that all three rutting tests can characterize the rutting performance of the studied mixes, despite the confounding effect of moisture sensitivity in the HWT test. To quantify the effect silo storage on rutting, the change in the rutting susceptibility was calculated for the different parameters: flow number from the unconfined RLT, rut depth at 10,000 passes from the HWT, and strain at 20,000 cycles from the confined RLT.

The percentage change was determined relative to the before-silo condition, shown in Figure 4.24. The relative change calculated using the flow number was high compared with the other two rutting parameters. For Mix C and Mix D, the change in the flow number was about 250% because of silo storage. The strain at 20,000 passes and the HWT test rut depth parameters provided a comparable measure of the relative increase in rutting resistance. The average change in these two rutting parameters—strain at 20,000 passes and rut depth at 10,000 passes—was between 10% and 60% across all four mixes. The effect of silo storage on Mix A and Mix C, with 5 hours and 6 hours of silo storage, respectively, was comparable to Mix B and Mix D, with 16 hours of silo storage. This observation indicates that silo storage time can be a significant factor even for short durations (i.e., 5 to 6 hours). The results also suggest a significant impact on mix properties within the first few hours in the silo.
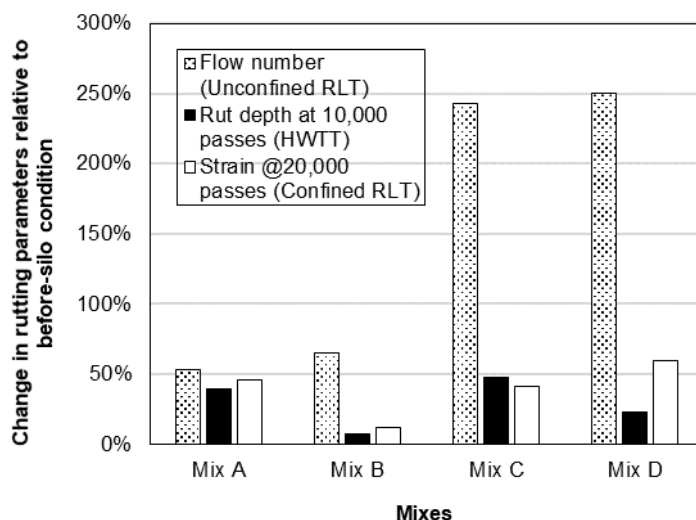
Figure 4.24: Change in the rutting parameters relative to the before-silo condition.

4.6   Overall Rutting Performance

The ranking of the mixes, based on their rutting resistance, was similar across all three tests. Overall, Mix C appears to have the best rutting performance of the four mixes, while Mix A and Mix B showed similarly low rutting performance. Mix C, exhibiting the best rutting performance, contained 20% RAP and 3% RAS. It is possible that the rutting resistance of Mix C can be attributed to the use of RAS in the mix, assuming that the RAS binder was blended with the RAP and virgin binders. Mix C also had a lower binder content of 5.2%.

Mix B, with 40% RAP, was expected to show high rutting resistance. However, the measured low rutting resistance of Mix B could be a result of using a soft virgin binder combined with incomplete blending between the RAP and virgin binders. It is interesting to note that 16 hours of silo storage time did not appear to enhance

the rutting resistance of Mix B significantly; the rut depth and strain at 20,000 passes only changed by an average of 10%, shown in Figure 4.24. Exactly why the rutting resistance of Mix B was not as high as expected and why it did not appear to improve with silo storage are difficult to determine, since the RAP stiffness was not known.

For Mix A, the use of a high dose of rejuvenator clearly resulted in a soft mix leading to reduced rutting resistance. The effect of silo storage on rutting was significant shown by an average 45% change in the rut depth and strain at 20,000 passes. Such a change could be an indication of the volatilization of the rejuvenator with silo storage and the additional blending and aging that occur inside the silo. The extent of blending and aging depends on many factors, including the properties and content of the RAP binder as well as the type and temperature of the silo.

4.7   Summary of Flexural Stiffness and Rutting Performance

Key observations from the flexural stiffness and rutting testing include the following:

- Mix A, with 50% RAP and a petroleum-based rejuvenator, and Mix B, with 40% RAP and a soft virgin binder, showed a lower modulus at higher temperatures compared with Mix C, with 20% RAP, 3% RAS, and a soft virgin binder, and Mix D, with 40% RAP and a biobased rejuvenator. This finding aligns with the HWT and RLT testing, which show that Mix A and Mix B were more susceptible to rutting.

- The high rejuvenator dose used in Mix A resulted in a low modulus at high temperatures, leading to a reduction in the rutting resistance.

- The use of RAS in Mix C and the use of a low rejuvenator dose in Mix D resulted in a relatively high modulus at high temperatures and increased rutting resistance compared with the other mixes.

- The increase in modulus with silo storage was dependent on the test frequency and the mix type. The maximum increase in stiffness was about 50% to 60% and at low test frequencies (i.e., high temperatures).

- Several tests and test parameters were successfully used to measure the rutting resistance of the mixes, including rut depth at 10,000 passes from the HWT, strain at 20,000 cycles from the confined RLT, and flow number and cycles at 5% strain from the unconfined RLT.

- Mix C, with RAS, showed the best rutting performance while Mix A showed the least rutting resistance, possibly due to the use of a high rejuvenator dose.

- The rutting resistance of all mixes increased with silo storage, except for the HWT test results for Mix D, which showed a slight decrease in rutting resistance. Mix A showed the most significant increase in rutting, with an average increase of about 45% in the rut depth at 10,000 passes and the strain at 20,000 cycles.

5 FRACTURE/CRACKING BEHAVIOR

5.1 Cracking Test Results

5.1.1 Semicircular Bending Test

The average flexibility index (FI) parameter calculated from a minimum of four replicate SCB test results is shown in Figure 5.1 for all mixes. The FI is a measure of both the fracture energy and the post-peak mix stiffness, and it is generally used to indicate the cracking resistance of the mix. High fracture energy and low stiffness both contribute to a high FI, and a high FI denotes better cracking resistance. The coefficient of variation for the FI for each mix and silo storage condition is shown in Table 5.1.

Table 5.1: Coefficient of Variation of Flexibility Index for Mixes and Silo Conditions

Mixes	A-0H	A-6H	B-0H	B-16H	C-0H	C-5H	D-0H	D-16H
Coefficient of Variation (COV) (%)	27.6	42.4	27.7	24.5	32.3	64.0	19.6	63.6

All mixes showed a drop in their flexibility indices due to silo storage. Mix B had a very high FI of 18.5 prior to silo storage; however, its FI went down to nearly 8 after 16 hours in the silo. Mix C and Mix D showed low FIs even before silo storage, and their FIs decreased further after silo storage. The fracture energy and post-peak slope values for all mixes were plotted to evaluate the effect of silo storage on each mix, shown in Figure 5.2. The post-peak slope (i.e., post-peak stiffness) increased significantly with silo storage. Silo storage also led to a reduction in the fracture energy of the mixes, except for Mix D.
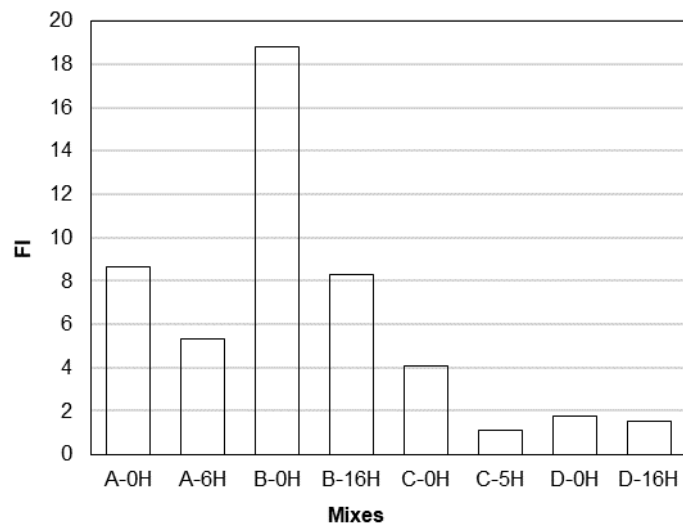
Figure 5.1: Flexibility index from SCB test for all mixes.
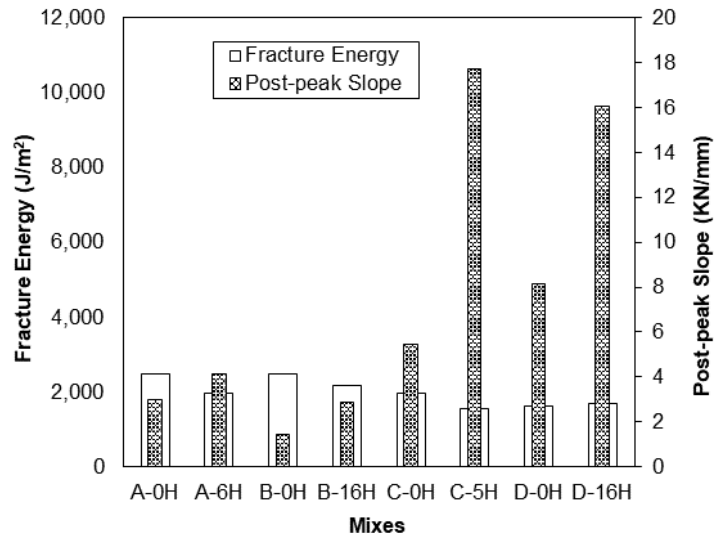
Figure 5.2: Fracture energy and post-peak slope from SCB test for all mixes.

The FI equation is a function of the fracture energy (area under the load versus deformation curve) and the post-peak load slope. Fracture energy is controlled by the specimen's strength and its ability to deform, and it is mainly a measure of the specimen deformation. Therefore, the FI can be simplified to provide an alternative measure of the mix flexibility by merely calculating the specimen deformation. The specimen deformation is measured as the total vertical displacement during the SCB test. However, to be consistent with the definition of the FI, the specimen deformation was defined as the total vertical displacement given by the intercept of the post-peak slope with the displacement axis ($l_{back-slope}$), shown in Figure 5.3.

Using this definition, the vertical displacement was calculated and plotted against the FI, shown in Figure 5.4. The correlation between the vertical displacement defined by $l_{back-slope}$ and the FI is very strong. This strong correlation indicates that the FI can be viewed as a measure of the specimen's ability to deform under a monotonic load and that it can potentially be replaced by a direct measure of the specimen deformation. However, the specimen deformation shown in Figure 5.3 requires the determination of the post-peak slope. The post-peak slope is sometimes difficult to calculate depending on the shape of the load-deformation curve and can be a source of error and variability of the FI. To avoid the need to determine the post-peak slope in calculating the vertical displacement, a simpler process is to measure the vertical displacement at a point corresponding to a given percentage of the peak load at the post-peak phase shown in Figure 5.3. The vertical displacement calculated at 75% peak load (l_{75}) was plotted against the FI in Figure 5.5, with a very strong correlation between vertical displacement and FI.

The previous discussion clearly shows that the FI can be considered a measure of the deformation ability of the mix. The mix deformation, including pre- and post-cracking, provides a direct measure of flexibility. Using a mix with a soft binder or increasing the air voids within the mix will lead to more deformation, resulting in a higher FI, which has been widely observed by other researchers *(19)*. However, the influence on air voids in improving FI is problematic because it is well-known that increased air voids result in poorer cracking performance, increased risk of moisture damage, poorer rutting performance, and poorer fatigue performance.
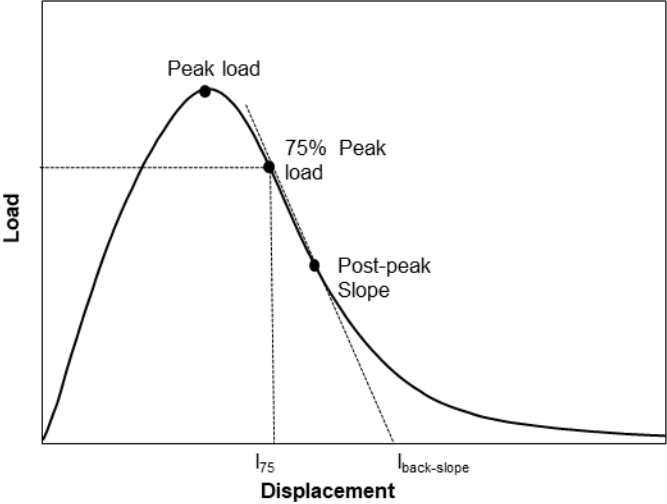
Figure 5.3: Load-displacement curve showing vertical displacement at 75% peak load (l$_{75}$) and at the intercept of the post-peak slope (l$_{back-slope}$).
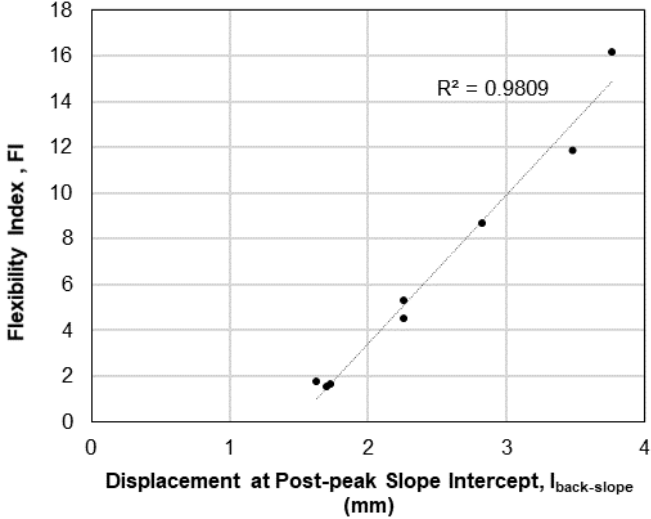
Figure 5.4: Flexibility index versus vertical displacement at post-peak slope intercept (l$_{back-slope}$) from SCB test.
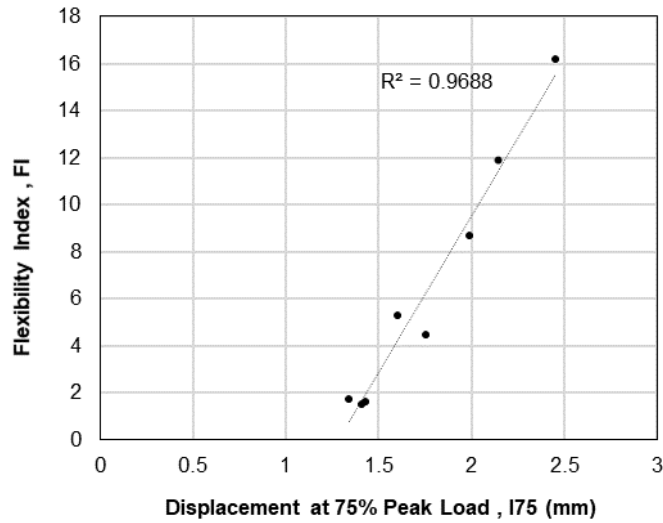
**Figure 5.5: Flexibility index versus vertical displacement at 75% peak load (l_{75})
from SCB test.**

5.1.2   IDEAL-CT Test

The average CT_{index} parameter was calculated from a minimum of three replicate IDEAL-CT test results for all the studied mixes, shown in Figure 5.6. The coefficient of variance (COV) of CT_{index} for each mixture and silo storage condition is given in Table 5.2. The COV of the CT_{index} results is much lower than the COV of the FI results. The CT_{index} followed a pattern like the FI where all mixes showed a reduction in the CT_{index} after silo storage. The fracture energy and post-peak stiffness from the IDEAL-CT test are shown in Figure 5.7. In general, the fracture energies calculated from the IDEAL-CT test are much higher compared with those calculated from the SCB test. The IDEAL-CT test uses unnotched specimens, and the larger fracture energy results from the IDEAL-CT test compared with the SCB test suggest that a great deal of energy is consumed during the plastic deformation and crack formation in the specimen prior to crack propagation. The fracture energy from the IDEAL-CT test does not show a clear trend with aging; hence, it does not seem to characterize the effect of aging on the cracking resistance of the mixes. The post-peak slope from the IDEAL-CT test showed an increase with aging, denoting higher mix stiffness.
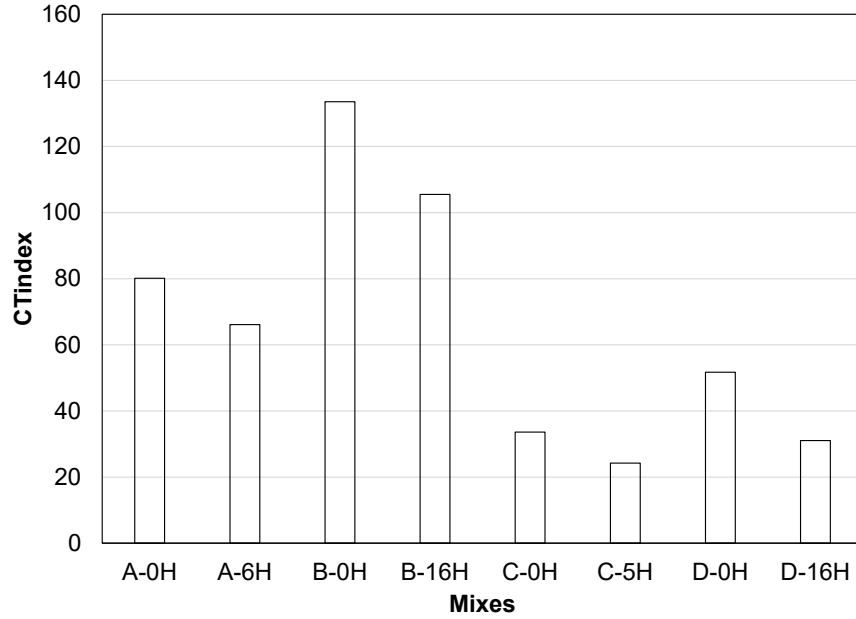
Figure 5.6: CT$_{index}$ from IDEAL-CT test for all mixes.

Table 5.2: Coefficient of Variation of CT$_{index}$ for Mixtures and Silo Conditions

Mixes	A-0H	A-6H	B-0H	B-16H	C-0H	C-5H	D-0H	D-16H
Coefficient of Variation (COV) (%)	22.5	22.9	17.4	20.5	26.8	24.8	5.7	24.2
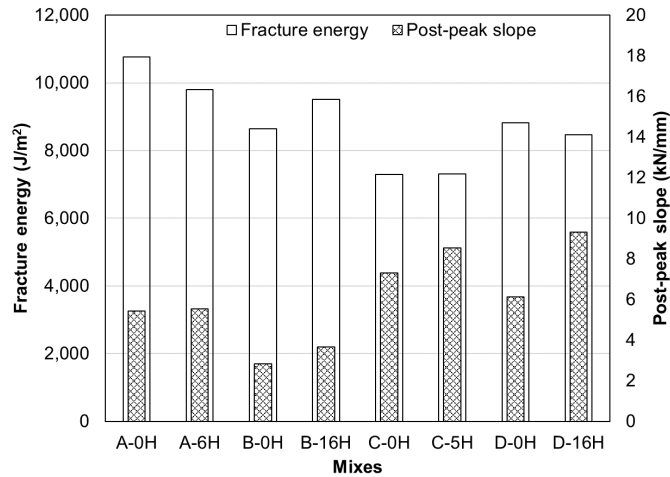
Figure 5.7: Fracture energy and post-peak slope from IDEAL-CT test for all mixes.

5.2 Analysis of Cracking Parameters

A comparison between the FI and CT$_{index}$ is shown in Figure 5.8 and reveals a very strong correlation between the two parameters. The calculation of both the FI and CT$_{index}$ depends primarily on the fracture energy and the post-

peak slope. There are many similarities between the formulation of the two parameters, which help explain the strong correlation. Other researchers have also reported the correlation between the two parameters *(18,19)*. The ranking of the mixes based on their cracking performance appears to follow a trend opposite to that of their rutting performance. Both the IDEAL-CT and the SCB tests provided the same ranking of the mixes in terms of their cracking resistance, where Mix A and Mix B showed higher cracking resistance compared with Mix C and Mix D.
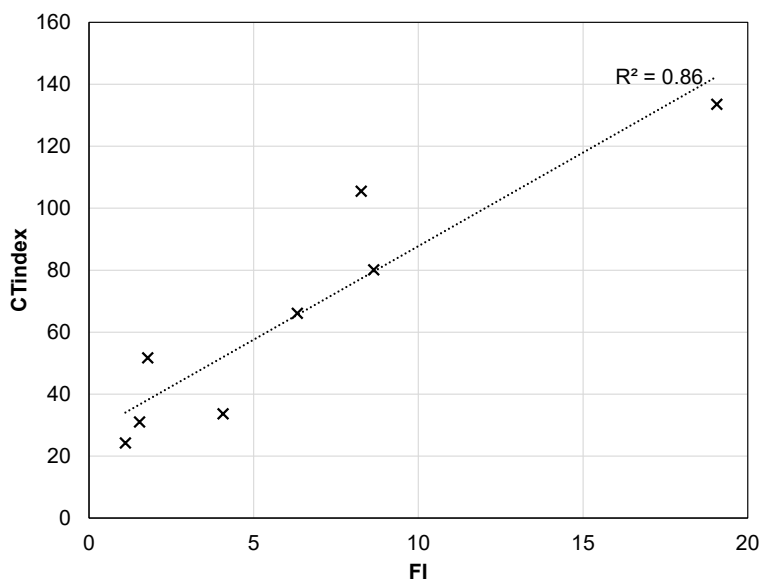
Figure 5.8: Correlation between FI and CT$_{index}$.

5.3   Effect of Silo Storage on Cracking Parameters

A statistical analysis using a t-test was conducted based on the CT$_{index}$ and FI to compare the cracking performance of the mixes before and after silo storage as measured by the two tests. The p-values, expressed as percentages, are shown Table 5.1. The change in cracking resistance with silo storage was statistically significant based on a 90% confidence limit for the FI for all the mixes but Mix D. The high p-value for the FI of Mix D was solely due to the high variability of the test results. The change with silo storage was only significant at that level for the CT$_{index}$ for Mixes B and D.

Table 5.3: P-Values for the Cracking Parameters Sensitivity to Silo Storage

Mixes	P-Value (CT$_{index}$) (%)	P-Value (FI) (%)
Mix A (50RAP-20RJ)	14	2.9
Mix B (40RAP)	7.5	0.1
Mix C (20RAP-3RAS)	13.6	0.6
Mix D (40RAP-0.7RJ)	0.1	19.2

Note: The mix code is %RAP-%RAS-%rejuvenating agent. RAP and RAS percentages are by mass of mix; rejuvenating agent percentage is by mass of total binder. Example: 50RAP-20RJ is 50% RAP, no RAS, and 20% rejuvenating agent.

To quantify the effect of silo storage on the cracking resistance of the mixes, the change in the different cracking parameters—FI from the SCB test and CT_{index} from the IDEAL-CT test—was calculated with aging, shown in Figure 5.9. The percentage change was determined relative to the before-silo condition. These results indicate that the effect of silo storage on the cracking parameters can be considerable, not only for Mix B and Mix D, which were allowed to sit for 16 hours in the silo, but also for Mix A and Mix C, which spent far less time in the silo. Generally, the effect of silo storage was more pronounced on the FI than the CT_{index}, except for Mix D, which showed high variability in its FI results. On average, the effect of silo storage led to a reduction across the two cracking parameters of about 30%.
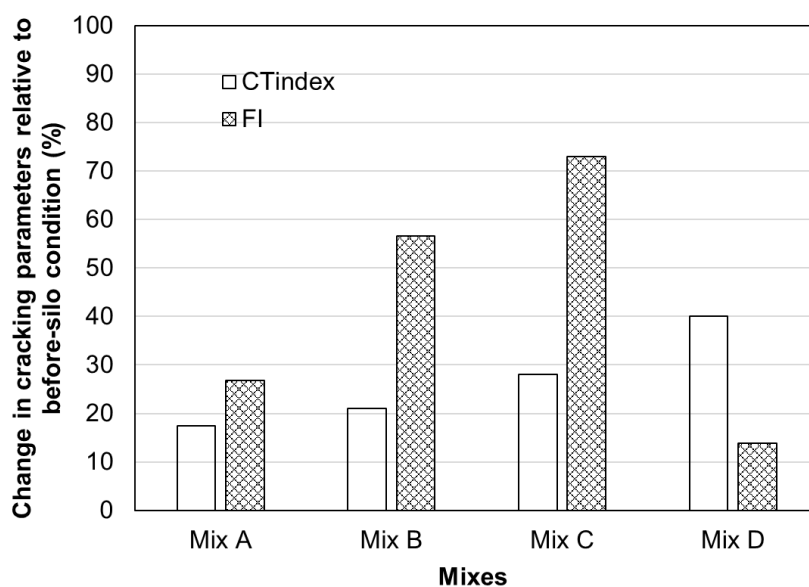
Figure 5.9: Change in the cracking parameters relative to the before-silo condition.

5.4   Impact of Stiffness on Cracking and Rutting Performance

The relationship between the stiffness of the mixes and their cracking and rutting performance was investigated. The overall performance of the mixes in terms of rutting and cracking resistance was captured by plotting the cycles at 5% strain versus the CT_{index}, shown in Figure 5.10. Mixes with high cracking resistance were associated with low rutting performance, whereas mixes with low cracking resistance was associated with good rutting performance. Among all the mixes, Mix B, with 40% RAP and a PG 58-28 binder, showed the highest cracking resistance and the lowest rutting resistance. On the other hand, Mix C, which incorporated RAS, showed the lowest cracking resistance and the highest rutting performance. The arrows in Figure 5.10 represent the direction of aging inside the silo. For all mixes, silo storage resulted in a decrease in the CT_{index}, indicating reduced cracking resistance accompanied by improved rutting resistance indicated by an increase in the cycles at 5% strain. However, the CT_{index} and the repetitions to 5% strain did not change consistently between the mixes. Mix B had a

steep decline in the cracking parameter with very little increase in the rutting parameter, while Mix C and Mix D had large increases in the rutting parameter with a small change in the cracking parameter. Mix A had little change of either parameter. The complex interactions of the characteristics of the base binders, the RAP and RAS binder characteristics, the interactions of those binders with rejuvenating agents when they were included, and the aging characteristics of all three or four binder ingredients (virgin, RAP, RAS, rejuvenating agent) likely played a role in these results.
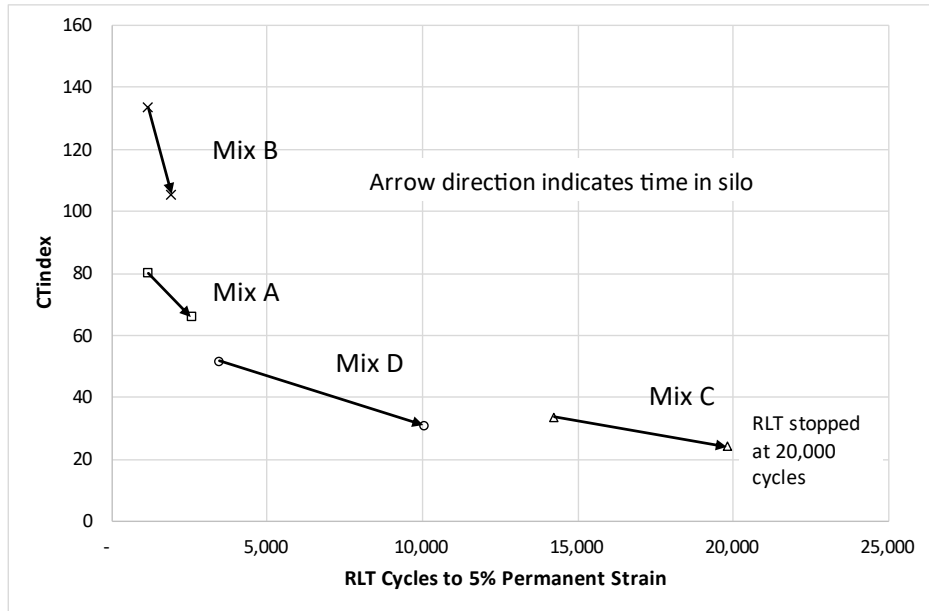
Note: Silo storage times are A: 6 hours, B: 16 hours, C: 5 hours, D: 16 hours.

Figure 5.10: Effect of aging on CT$_{index}$ and cycles at 5% strain.

The relationship between stiffness and cracking was investigated by plotting the flexural stiffness at 20°C (68°F) and 10 Hz (E50) versus the IDEAL-CT strength, shown in Figure 5.11. The IDEAL-CT strength represents the peak stress that can be obtained directly using the load-deformation curve. The CT$_{index}$ did not appear to be very well correlated with the flexural stiffness (E50), shown in Figure 5.12.
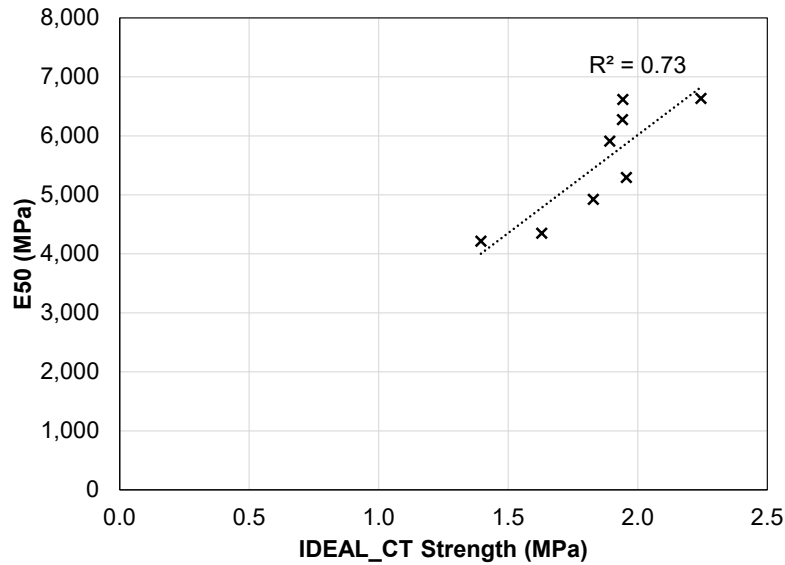
Figure 5.11: Flexural stiffness at 20ºC (68ºF) and 10Hz (E50) versus IDEAL-CT strength.
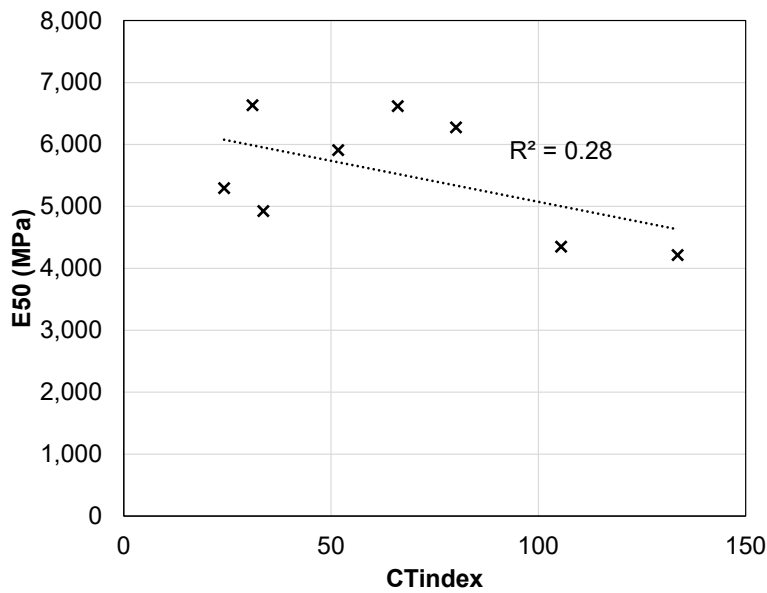
Figure 5.12: Flexural stiffness at 20ºC (68ºF) and 10Hz (E50) versus CT_{index}.

5.5 Summary of Cracking Performance

Key observations from the SCB and IDEAL-CT testing include the following:

- The variability of the air void contents of the SCB specimens was high, as allowed under the version of the test applicable when specimens were made, which introduced more variability into the results.

- The FI from the SCB test and the CT_{index} from the IDEAL-CT test showed strong correlation.

- The cracking resistance of the mixes decreased with silo storage, as measured by the FI and CT_{index}.

- The cracking resistance of the mixes was inversely related to the rutting resistance. Mix C, with RAS, had the highest rutting resistance and lowest cracking resistance of all mixes. On the other hand, Mix B, with 40% RAP and a rejuvenator, showed the lowest rutting resistance and highest cracking resistance.

- The FI was shown to correlate very well with the specimen's vertical displacement, particularly the displacement given by the intercept of the post-peak slope. This indicates that the FI can be viewed as a direct measure of the specimen's ability to deform under load.

- The CT_{index} decreased and the RLT repetitions to 5% strain increased with silo aging. However, the amount of change in each parameter varied greatly between the four mixes.

- The flexural stiffness (E50) at $20^{\circ}C$ ($68^{\circ}F$) and 10Hz showed good correlation with the IDEAL-CT strength, indicating that the IDEAL-CT test can be used to provide a measure of the mix stiffness.

- No correlation was found between the E50 parameter and the CT_{index}.

6 FATIGUE BEHAVIOR

6.1 Flexural Beam Test Results

The flexural beam test was conducted at three different strain levels. The fatigue life was determined, according to AASHTO T 321, to be the number of cycles corresponding to the point at which the product of the stiffness and loading cycles is at the maximum. Using a log-log scale, the fatigue life was fitted using a linear regression model and plotted against the strain level, which is referred to as a Wöhler curve, and is shown in Figure 6.1 to Figure 6.4 for all four mixes. At high strain levels, the silo storage resulted in a decrease in fatigue life. The increase in mix stiffness due to silo storage resulted in an increase in the applied stress during a strain-controlled loading and a subsequent reduction in the fatigue life of the mix. At low strain levels, where the mixes are subjected to low stresses, the fatigue life appears to increase with silo storage. As noted previously, complex interactions are at work that are likely causing these changes observed with silo storage, including the following:

- Mobilization of the RAP binder and better blending of the RAP binder with the virgin binder, producing higher binder contents that should increase fatigue life.

- Stiffening of the binder because of the increased RAP binder content, and aging of the virgin binder and rejuvenator (if present), which should reduce controlled-strain fatigue life.

- Relative amounts of virgin binder, RAP binder, and rejuvenator in the mix that are aging at different rates as they are also diffusing into each other.

With silo storage (i.e., aging), the fatigue life becomes more sensitive to the applied strain, as identified by an increase in the slope of the fatigue life versus strain line becoming steeper. This indicates that these mixes will have longer fatigue lives at smaller strains, typical of thicker overlays and asphalt layers, and shorter fatigue lives at larger strains, typical of thin overlays. Aging increases the stiffness of the mix as well. So in thick asphalt layers and overlays, the tensile strain becomes less under a traffic load, and the fatigue life, at a given strain, becomes longer, compared with the unaged mix.
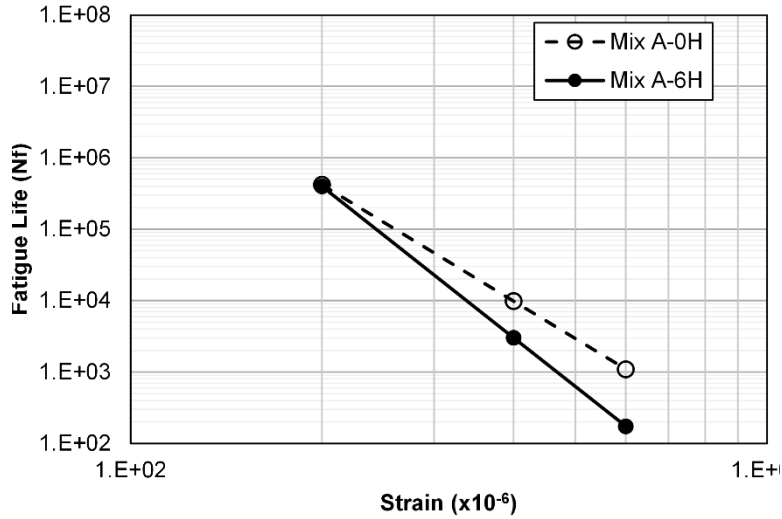
Note: The mix code is %RAP-%RAS-%rejuvenating agent. RAP and RAS percentages are by mass of mix; rejuvenating agent percentage is by mass of total binder. Example: 50RAP-20RJ is 50% RAP, no RAS, and 20% rejuvenating agent.

Figure 6.1: Fatigue life versus strain for Mix A (50RAP-20RJ).
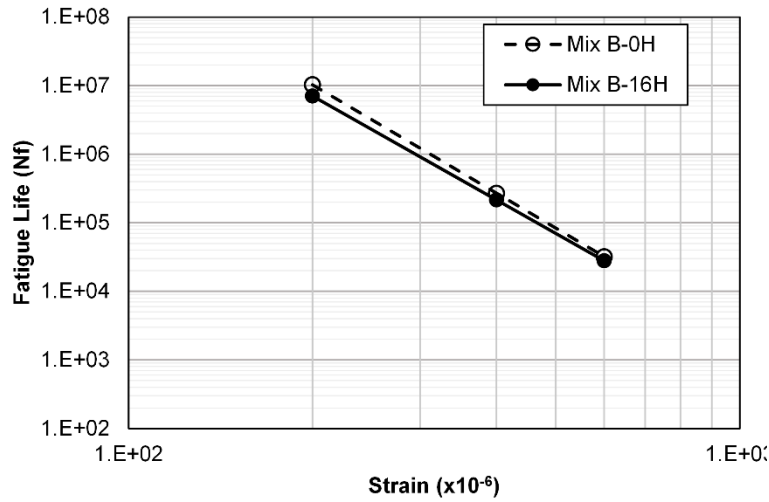
Note: The mix code is %RAP-%RAS-%rejuvenating agent. RAP and RAS percentages are by mass of mix; rejuvenating agent percentage is by mass of total binder. Example: 50RAP-20RJ is 50% RAP, no RAS, and 20% rejuvenating agent.

Figure 6.2: Fatigue life versus strain for Mix B (40RAP).
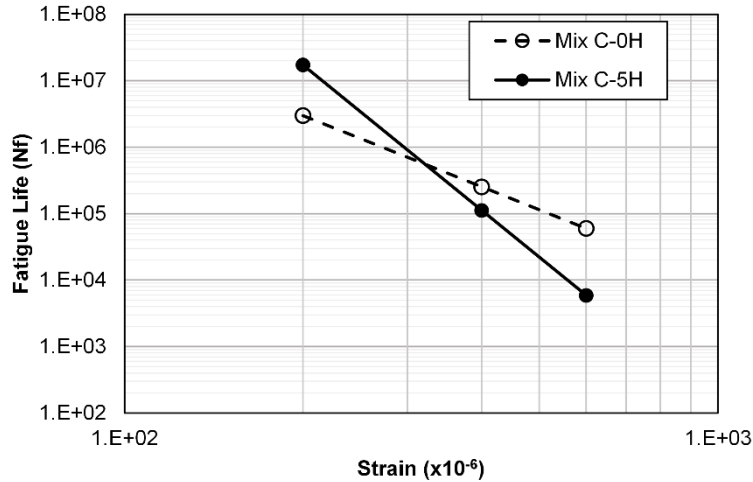
Note: The mix code is %RAP-%RAS-%rejuvenating agent. RAP and RAS percentages are by mass of mix; rejuvenating agent percentage is by mass of total binder. Example: 50RAP-20RJ is 50% RAP, no RAS, and 20% rejuvenating agent.

Figure 6.3: Fatigue life versus strain for Mix C (20RAP-3RAS).
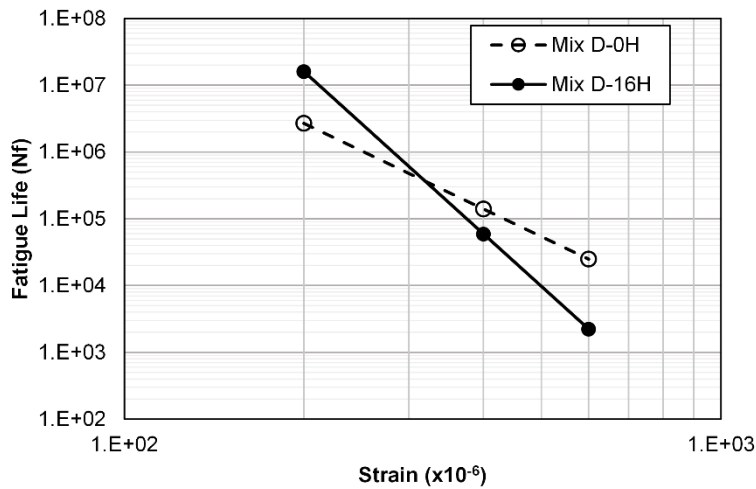
Note: The mix code is %RAP-%RAS-%rejuvenating agent. RAP and RAS percentages are by mass of mix; rejuvenating agent percentage is by mass of total binder. Example: 50RAP-20RJ is 50% RAP, no RAS, and 20% rejuvenating agent.

Figure 6.4: Fatigue life versus strain for Mix D (40RAP-0.7RJ).

Using the linear relationships between fatigue life and strain, strain levels that will result in a fatigue life of 1 million cycles and 250,000 cycles were estimated and plotted in Figure 6.5. These strain levels indicate the fatigue performance of the mixes at low and high strain levels, where the low strain level is represented by the strain at 1 million cycles and the high strain level is represented by the strain at 250,000 cycles. The strain levels are a means to compare the mixes and assess the effect of silo storage. A higher strain level at the same number of loading cycles indicates better fatigue performance. Mix A had very low fatigue performance compared with

the other mixes, possibly due to its low binder content and the high rejuvenator dose, which resulted in a low virgin binder content.
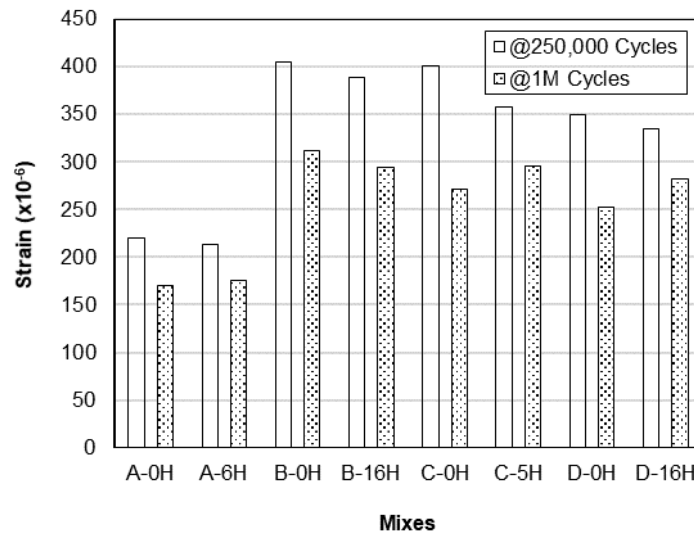
Figure 6.5: Strain at 250,000 cycles and 1 million cycles for all mixes.

6.2 Correlation Between Cracking and Fatigue

To investigate whether the cracking resistance tests—the I-FIT and IDEAL-CT tests—can indicate fatigue performance, the strain at 250,000 cycles was plotted versus the average FI, shown in Figure 6.6, and the average CT_{index}, shown in Figure 6.7, and the strain at 1M cycles was plotted versus the FI, shown in Figure 6.8, and the CT_{index}, shown in Figure 6.9. The FI and CT_{index} did not capture the differences between the mixes based on their fatigue performance. Mix A shows a relatively high FI and CT_{index} but considerably low fatigue performance compared with the other mixes. The performance of Mix A was largely governed by the high dose of rejuvenator, which led to a reduced mix stiffness and a low virgin binder content. The low stiffness exhibited by Mix A is reflected in the high FI and CT_{index}, while its poor fatigue performance could be attributed in part due to its low binder content and the rejuvenating agent. The results for strain at 1 million cycles showed a similar lack of correlation with FI and CT_{index}.
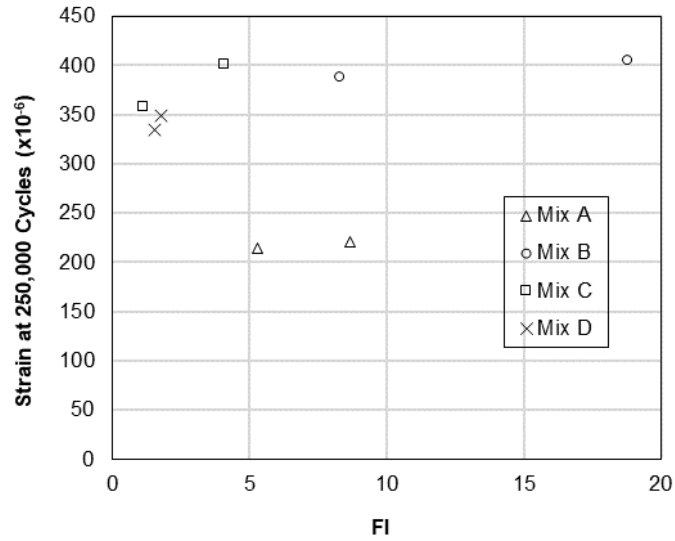
Figure 6.6: Strain at 250,000 cycles from flexural beam test versus FI from I-FIT test for aged and unaged mixes.
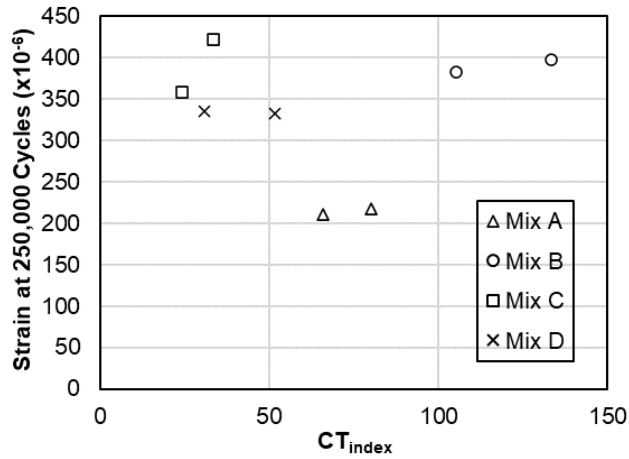
Figure 6.7: Strain at 250,000 cycles from flexural beam test versus CT_{index} from IDEAL-CT test for aged and unaged mixes.
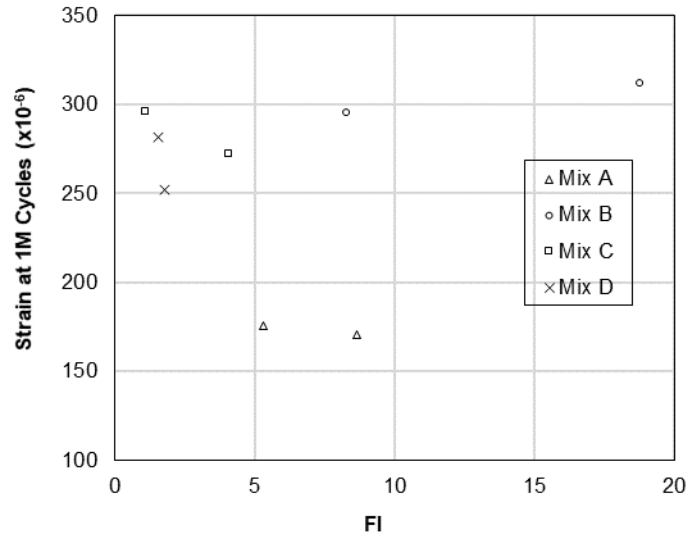
Figure 6.8: Strain at 1 million cycles from flexural beam test versus FI from I-FIT test for aged and unaged mixes.
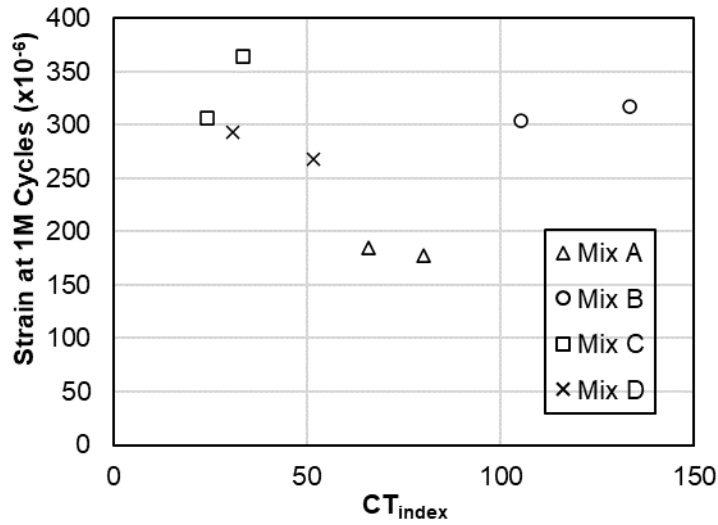
Figure 6.9: Strain at 1 million cycles from flexural beam test versus CT$_{index}$ from IDEAL-CT test for aged and unaged mixes.

6.3 Summary of Fatigue Performance

Key observations from the flexural beam testing include the following:

- The strain-controlled flexural beam test showed that silo storage led to a reduction in the fatigue life of all mixes, particularly at high strain levels, while fatigue life was increased with silo storage for three of the four mixes at low strain levels.

- No correlation could be established between the cracking parameters—FI and CT_{index}—and the strain at a fatigue life of 250,000 cycles and 1 million cycles. The variability of the air voids of the FI specimens was high, which should be considered when interpreting these results, but which is not expected to change the conclusion.

7 FINE AGGREGATE MATRIX MIX TESTING

Fine aggregate matrix (FAM) specimens were tested in a dynamic shear rheometer (DSR) to assess their fatigue cracking resistance using linear amplitude sweep (LAS) loading. The material for FAM specimens was obtained by screening plant-produced mix on the 2.36 mm sieve. FAM mixes were compacted into 150 mm diameter by 50 mm high specimens in a Superpave gyratory compactor. Air void contents ranged from 10% to 12%. Previous studies on FAM mixes have shown that the effect of the variation of air voids within this target range is insignificant *(27)*. Cylindrical FAM mix specimens measuring 12 mm in diameter were cored from the compacted specimens. A minimum of three specimens for each mix type was tested.

The LAS testing procedure was conducted at a temperature of 25°C (77°F), based on AASHTO TP101, with modifications to account for the FAM mix testing. To determine the undamaged properties of the mix, a frequency sweep testing was performed covering a range of frequencies from 0.1 to 25 Hz at a strain level of 0.002%. The strain level of 0.002% was selected to ensure the material remained within the linear viscoelastic region *(28)*. Using the results of the frequency sweep, a parameter α was calculated that represents the damage rate relative to undamaged properties as defined by the viscoelastic continuum damage model (VECD) theory. Following the frequency sweep testing, the strain was increased with time using a linear log scale from 0.002% to 0.6% at a constant frequency of 10 Hz. An increase in the strain rate with time based on a linear log scale allowed for more loading cycles at lower strain rates and fewer loading cycles at higher strain rates. Using more loading cycles at lower strain rates ensured that sufficient damage occurred in the specimen before higher strain rates were applied.

7.1   The Viscoelastic Continuum Damage Model

The VECD is based on Schapery's work potential theory *(29)*, shown in Equation 7.1:

$$\frac{dD}{dt} = \left(\frac{dW}{dD}\right)^{\alpha} \tag{7.1}$$

Where:

D = Damage

t = time

W = work performed

α = material constant

The work potential theory establishes a relationship between the damage rate and the rate of work performed. A parameter α is defined, which can be directly obtained using the slope of the log-log plot of the storage modulus versus frequency. The relationship between the storage modulus and the frequency is defined by Equation 7.2:

$$log\, G'(\omega) = m(log\, \omega) + b \tag{7.2}$$

Where:

G' = the storage modulus

ω = the test frequency

m = the slope of the regression line

b = a constant

The parameter α is then be calculated using Equation 7.3:

$$\alpha = 1/m \qquad\qquad (7.3)$$

Using the LAS test results, the accumulation of damage intensity over the loading cycles (N) is calculated using Equation 7.4:

$$D(t) \cong \sum_{i=1}^{N}[\pi I_D \gamma_o^2(|G^*|sin\delta_{i-1} - |G^*|sin\delta_i)]^{\frac{\alpha}{1+\alpha}}(t_i - t_{i-1})^{\frac{1}{1+\alpha}} \qquad\qquad (7.4)$$

Where:

$D(t)$ = the damage intensity at time t

I_D = the initial complex shear modulus, MPa

γ_o = the applied shear strain

$|G^*|$ = the complex shear modulus, Mpa

The relationship between damage intensity and the loss modulus ($|G^*|sin\delta$) is fitted using the power law curve shown in Equation 7.5 *(30)*:

$$|G^*|sin\delta = C_0 - C_1 D^{C_2} \qquad\qquad (7.5)$$

Where:

Co = the average $|G^*|sin\delta$ at the initial strain rate

C_1 and C_2 = curve fitting coefficients

According to AASHTO TP101, the failure is defined as a 35% decrease in the undamaged value of $|G^*|sin\delta$. However, this study proposes using the peak phase angle as an alternative failure criterion to replace the 35% decrease criterion defined in AASHTO TP101.

The relationship between fatigue life (N_f) and strain rate is then written as Equation 7.6:

$$N_f = A(\gamma_o)^{-B} \qquad\qquad (7.6)$$

With the coefficients A and B given by Equations **7.7** and 7.8:

$$A = \frac{f(D_f)^k}{k(\pi I_D C_1 C_2)^\alpha} \qquad (7.7)$$

$$B = 2\alpha \qquad (7.8)$$

Where:

$k = 1 + (1 - C_2)\,\alpha$

f = loading frequency at 10 Hz

D_f = the damage intensity at failure, defined at peak phase angle

7.2   Fatigue Life

The complex modulus and phase angle were measured during the FAM mix testing, at different strain levels. A plot of the complex modulus and phase angle versus strain for one of the specimens from Mix A-0H is shown as an example in Figure 7.1. The complex modulus curve can be generally divided into three regions. The first region is characterized by a decrease in the complex modulus at a decreasing rate. The onset of the second zone marks the failure of the specimen, with a sharp drop in the complex modulus. This zone is then followed by a third zone where the complex modulus continues to decrease, though the decrease occurs at a slow rate.

The variation of the phase angle appears to follow the same pattern of regions noted in the complex modulus curve. In the first region, the phase angle increases consistently at a decreasing rate until it reaches a maximum. The maximum phase angle signifies the failure of the specimen and the start of the second region. The third region shows a continuous decrease in the phase angle, though the decrease occurs at a slow rate. In some instances, such as the example in Figure 7.1, the phase angle will drop for a few cycles and then increase abruptly again for the next few cycles before it starts to decrease steadily until it reaches a plateau. The decrease in the modulus follows a linear slope followed by a sudden decrease in the modulus denoting failure. The sudden decrease in the modulus coincides with the point at which the phase angle reaches its first maximum, shown in Figure 7.1. The peak phase angle was used to define fatigue failure, and the fatigue life was calculated accordingly using the VECD model analysis.
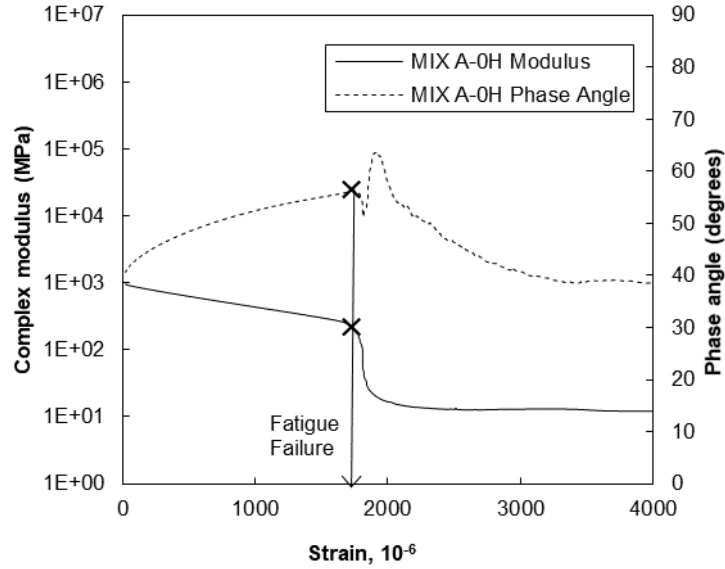
Figure 7.1: A plot of the modulus and phase angle versus strain for Mix A-0H showing the fatigue life at peak phase angle.

The fatigue life was calculated at different strains using the VECD model described above, shown in Figure 7.2 through Figure 7.5, for the four mixes. The effect of silo storage on fatigue life was evident, particularly for FAM Mix A and FAM Mix C, which had the least amount of silo storage time. For Mix A and Mix C, the mixes subjected to silo storage showed a steeper slope, indicating a higher rate of deterioration in fatigue life with increasing strain, compared with the before-silo mixes. This indicates that the effect of silo storage on fatigue life was more pronounced at higher strain levels, which agrees with the findings from the flexural beam test results.

A direct comparison between strain levels and fatigue life obtained through FAM mix testing and flexural beam testing is not valid due to the different compositions of the mixes (FAM versus full mixes), and the different configuration of the tests (torsion for the FAM mix LAS test and tension for the flexural beam test). Nevertheless, both the FAM mix test and the full mix flexural beam test caused damage under repeated loading at intermediate temperatures and both test results showed similar trends with respect to the effect of silo storage and the variation of fatigue life with strain rate for both the before- and after-silo conditions.
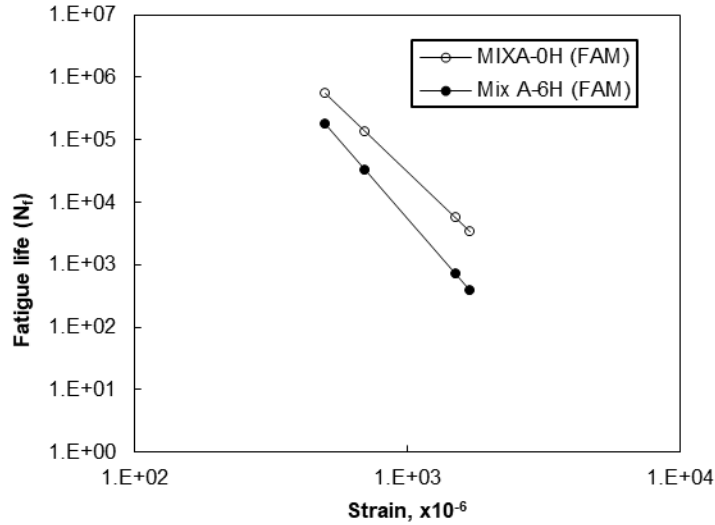
Note: The mix code is %RAP-%RAS-%rejuvenating agent. RAP and RAS percentages are by mass of mix; rejuvenating agent percentage is by mass of total binder. Example: 50RAP-20RJ is 50% RAP, no RAS, and 20% rejuvenating agent.

Figure 7.2: Fatigue life versus strain for FAM Mix A (50RAP-20RJ).
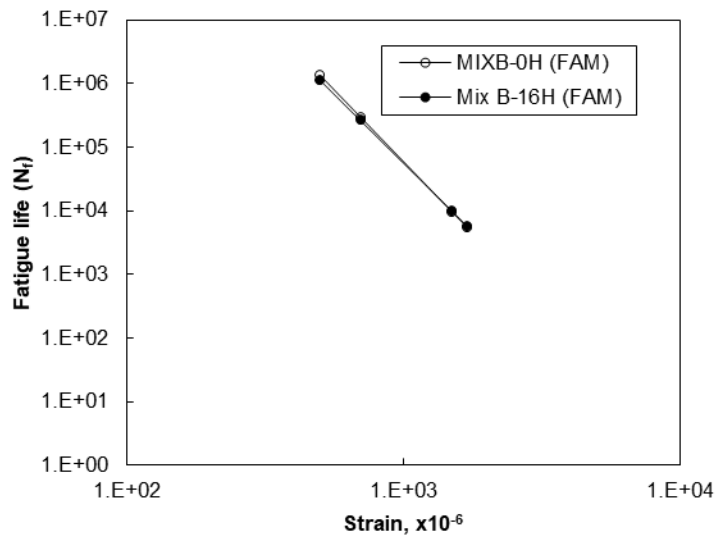
Note: The mix code is %RAP-%RAS-%rejuvenating agent. RAP and RAS percentages are by mass of mix; rejuvenating agent percentage is by mass of total binder. Example: 50RAP-20RJ is 50% RAP, no RAS, and 20% rejuvenating agent.

Figure 7.3: Fatigue life versus strain for FAM Mix B (40RAP).
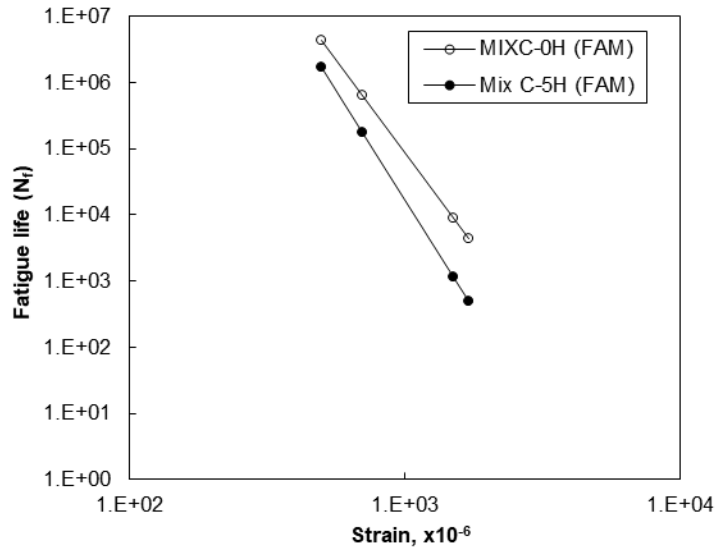
Note: The mix code is %RAP-%RAS-%rejuvenating agent. RAP and RAS percentages are by mass of mix; rejuvenating agent percentage is by mass of total binder. Example: 50RAP-20RJ is 50% RAP, no RAS, and 20% rejuvenating agent.

Figure 7.4: Fatigue life versus strain for FAM Mix C (20RAP-3RAS).
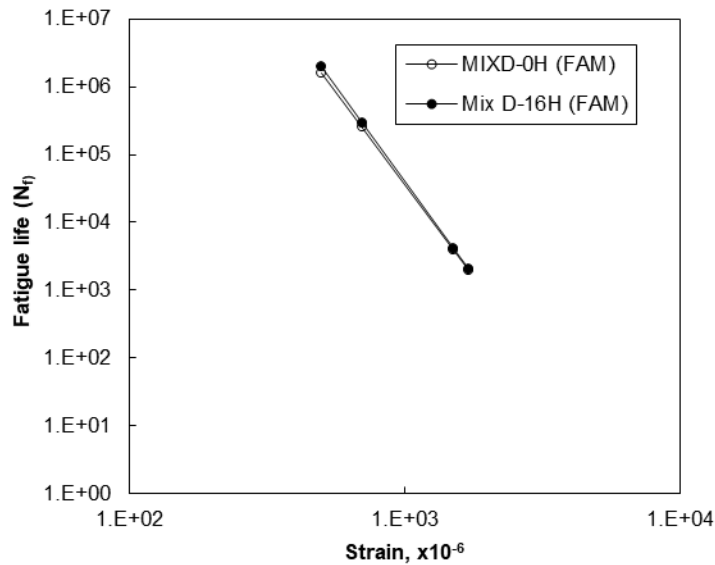
Note: The mix code is %RAP-%RAS-%rejuvenating agent. RAP and RAS percentages are by mass of mix; rejuvenating agent percentage is by mass of total binder. Example: 50RAP-20RJ is 50% RAP, no RAS, and 20% rejuvenating agent.

Figure 7.5: Fatigue life versus strain for FAM Mix D (40RAP-0.7RJ).

7.3   Fatigue Performance of FAM Mixes

The fatigue performance of the FAM mixes can also be compared using measures other than the fatigue life. The failure strain is defined as the strain corresponding to the peak phase angle. The abrupt decrease in the modulus corresponding to the peak phase angle was calculated for all mixes and plotted in Figure 7.6. Silo storage generally

caused a decrease in the failure strain denoting lower fatigue performance. Mix A showed the lowest fatigue resistance compared with the other mixes, a result that is consistent with the flexural beam test. In contrast to the other three mixes, Mix D showed a slight increase in failure strain with silo storage. However, such an increase was within the coefficient of variation of the results and therefore was not considered significant. It should be emphasized that the failure strain calculated in Figure 7.6 is specific to the pattern of loading that was used in the test and should not be considered indicative of failure under a general state of loading. The failure strain, however, can be directly obtained from the FAM test results without the need to undergo further analysis.
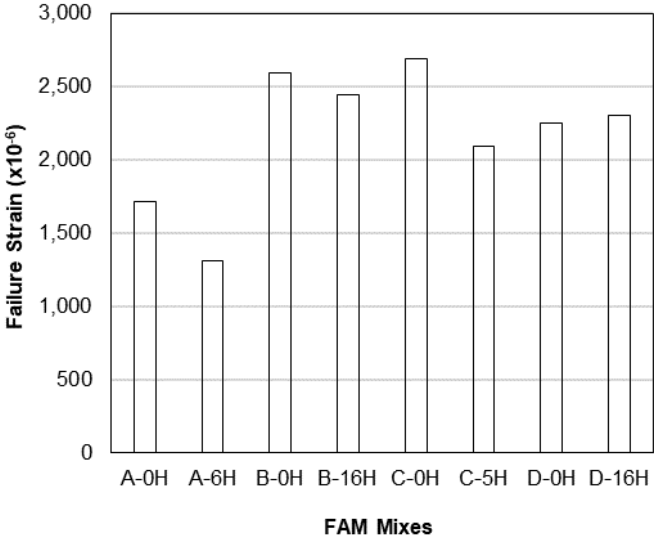
Figure 7.6: Fatigue failure strain for all FAM mixes.

Another fatigue parameter that can be used in lieu of fatigue life and failure strain is strain at 250,000 or 1 million cycles. Using the linear relationship between log fatigue life and log strain developed in Figure 7.2 through Figure 7.5, the strain corresponding to a fatigue life of 250,000 and 1 million cycles was calculated. Figure 7.7 shows that for Mix A and Mix B the strain at 250,000 and 1 million cycles tended to decrease with silo storage, indicating lower fatigue performance. For Mix C and Mix D, the strain at 250,000 cycles and 1 million cycles showed mixed results for silo storage compared with no silo storage as did the flexural beam fatigue tests. In addition, Mix A shows the lowest strain among all mixes, indicating the least fatigue performance.
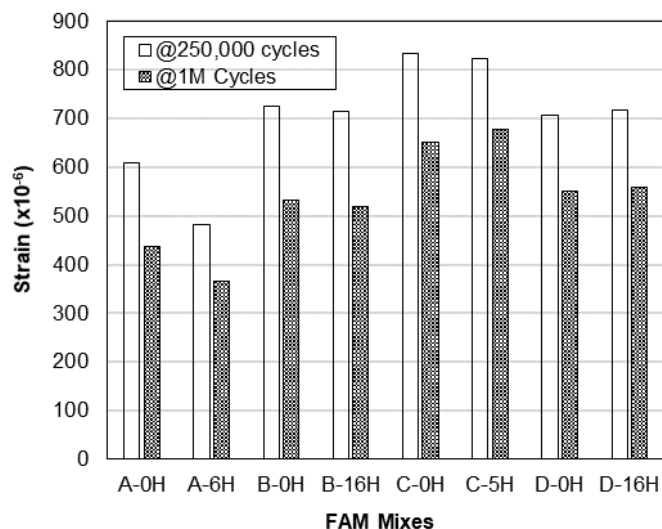
Figure 7.7: Fatigue failure strain at 250,000 and 1 million cycles for FAM mixes.

These results show that all the fatigue parameters—fatigue life, failure strain, strain at 1 million cycles, and strain at 250,000 cycles—provided similar ranking of the mixes and were able to capture the effect of silo storage on performance. In addition, the poor fatigue performance of Mix A was captured by all fatigue parameters. The following discussion compares fatigue performance measured using the FAM mix testing and the flexural beam test.

7.4   Correlation Between FAM Mix Testing and Flexural Beam Testing

Both FAM mix testing and flexural beam tests apply cyclic loading to measure the resistance of the mix against fatigue failure. The distinct differences between the two types of tests were previously discussed. Despite these differences, both tests appear to be capable of characterizing the fatigue performance of the mixes and assessing the impact of silo storage on fatigue properties.

FAM mix testing is faster and uses less material compared with the flexural beam test. For these reasons, it is a candidate for use in lieu of flexural beam testing, if it provides similar results. It was therefore important to investigate the relationship between the two fatigue tests using the fatigue parameters previously discussed. The strain at a fatigue life of 250,000 cycles was determined for all mixes using the flexural beam test results, presented in Chapter 4. As discussed in the previous section, the failure strain, and the strain at 250,000 cycles can be used to measure the fatigue performance of FAM mixes. Figure 7.8 shows the relationship between the strain at a fatigue life of 250,000 cycles from the FAM mix test and the flexural beam test. Generally, a fair correlation existed between the strain at 250,000 cycles for the two tests as shown by the R^2 value.
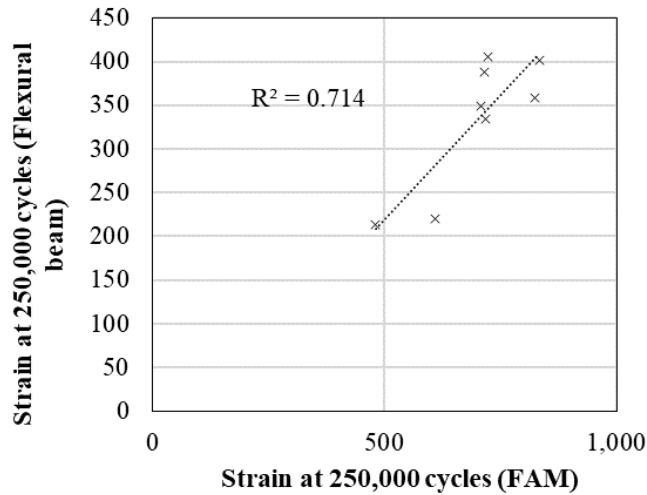
Figure 7.8: Strain at 250,000 cycles using both the FAM and the flexural beam tests.

The relationship between strain at failure from the FAM test and the strain at 250,00 cycles from the flexural beam test was investigated as shown in Figure 7.9. A good correlation was shown between these two parameters, indicating that the FAM test can be used successfully to provide an indicative measure of fatigue performance that is consistent with the flexural beam test.
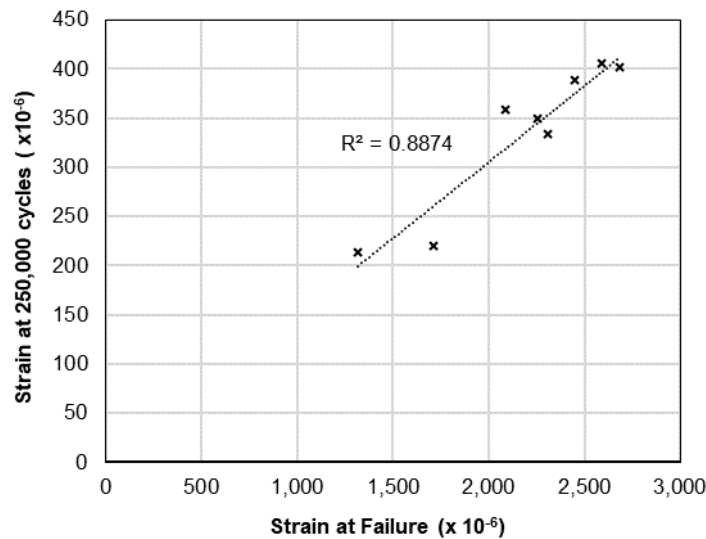
Figure 7.9: Failure strain from FAM mix testing versus strain at 250,000 cycles from flexural beam test.

7.5   FAM Mix Modulus Master Curves

In addition to the fatigue testing, the FAM mixes were also tested to determine their modulus at different temperatures and frequencies using a DSR by conducting at temperature-frequency sweep. Frequency sweep

testing was performed at four different temperatures—4ºC (39.2ºF), 21ºC (69.8ºF), 37ºC (98.6ºF), and 54ºC (129.2ºF)—over a range of frequencies between 0.1 Hz and 25 Hz, according to AASHTO T 342.

The modulus master curves of the FAM mixes before silo storage were constructed at a reference temperature of 20ºC (68ºF), shown in Figure 7.10. FAM Mix A and FAM Mix B showed lower modulus values at higher temperatures (i.e., lower frequencies) compared with FAM Mix C and FAM Mix D. This finding is consistent with the flexural beam testing of the full-graded mixes presented earlier in Section 3.1. The ranking of the FAM mixes based on their modulus values at higher temperatures agreed with the full-graded mix testing.

The modulus master curves of the FAM mixes after silo storage were also determined. The effect of silo storage was assessed by normalizing the modulus master curves obtained for the mixes after silo storage with respect to the modulus master curves obtained for the mixes before silo storage. The normalized master curves are shown in Figure 7.11. A notable increase in modulus with silo storage is noted for FAM Mix A and FAM Mix C, while FAM Mix B showed relatively less increase in modulus. FAM Mix D did not appear to show any increase in modulus with silo storage and showed a slight decrease in modulus with silo storage. It was not clear why the testing of FAM Mix D did not capture the expected increase in modulus that was evident with the flexural testing of the full-graded mixes.

The results of the FAM mix stiffness testing clearly indicate that FAM mixes can be used to provide an indication of the stiffness of the full-graded mixes. The FAM mix testing also captured the increase in mix stiffness with silo storage, except for Mix D.
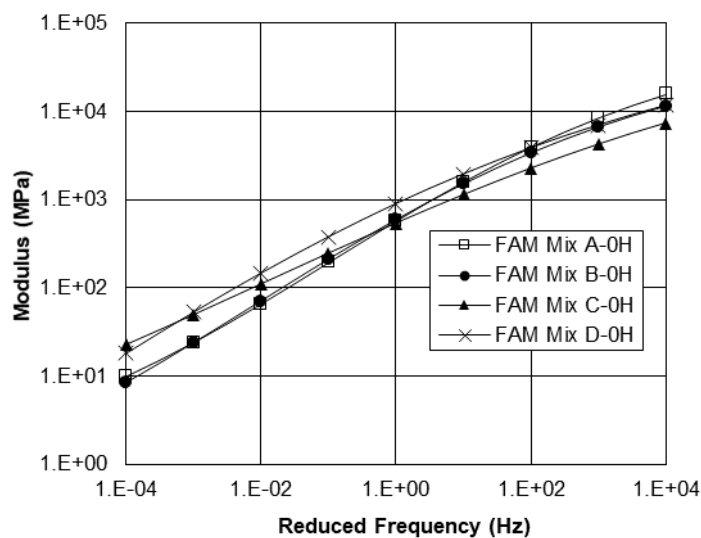
Figure 7.10: Modulus master curves for the FAM mixes.
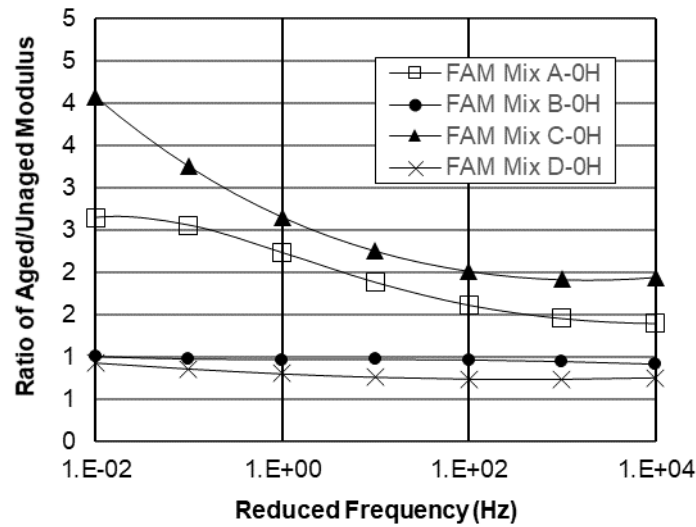
Figure 7.11: Effect of silo storage on the modulus master of FAM mixes normalized to unaged stiffness for each mix.

7.6 Summary of Fine Aggregate Matrix Testing

Key observations from the FAM testing include the following:

- Using LAS testing of FAM mixes, the fatigue life of FAM mixes was determined using the VECD model.

- The fatigue life decreased with silo storage at 250,000 cycles and 1 million cycles for Mix A and Mix B, and Mix C and Mix D showed mixed results.

- The failure strain, defined at the peak phase angle, decreased with silo storage for all FAM mixes at high strain levels while the results were mixed at low strain levels.

- The failure strain from the FAM mix testing showed good correlation with the strain at 250,000 cycles from the flexural beam test.

- Using temperature-frequency sweep testing of FAM mixes, the modulus master curves of the FAM mixes showed ranking of the mixes similar to that of the modulus master curves of the full-graded mixes. This indicates that FAM mix testing can be used to provide insight into the stiffness of the full-graded mixes.

8 CONCLUSIONS AND PRELIMINARY RECOMMENDATIONS

8.1 Summary

Short-term aging of asphalt mixes represents aging that takes place during mixing, transportation, and placement. During production, asphalt plants can directly load mix into trucks for transport to the paving site or store mix in silos for a few to many hours before transporting it to the job site. Current standard specifications do not limit silo storage time. The ability to store mix in a silo is essential for maintaining a steady supply of hot mix to the paver during paving, considering available hours to mix, mixing plant and paving productivity rates, and breaks in paving caused by lane changes and equipment and trucking breakdowns.

The aging that takes place inside the silo is not accounted for during the mix design process, and it is not strictly accounted for in quality assurance procedures. In mixes that incorporate high amounts of RAP/RAS, additional blending can occur between the recycled and virgin binders while inside the silo. Moreover, high RAP or RAS mixes mostly include petroleum or bioderived additives called rejuvenators, depending on their chemical composition, to restore the properties of the mix. These rejuvenators may undergo physical or chemical changes during the silo storage, leading to further changes in the mix properties. Silo storage also increases aging of the virgin binder in the mix.

This study included a literature review and extensive performance-related testing to assess the effect of silo storage on the stiffness, rutting, cracking, and fatigue properties of four high RAP or RAS mixes, including FAM mixes and full-graded mixes.

Key points from the literature review include the following:

- Addition of RAP/RAS increases mix stiffness and reduces fatigue cracking resistance at a given tensile strain level, which generally matches performance of the mix when used in thin overlays or new pavement layers. When used in thicker overlays and new pavement layers, the increased stiffness will decrease the tensile strain while also decreasing the fatigue life at a given tensile strain, and the two counteracting influences need to be considered through mechanistic pavement structural analysis. Addition of RAP/RAS will reduce low-temperature and block cracking performance. Several mitigation measures can be taken to improve fatigue performance of mixes with RAP/RAS at a given strain and low-temperature and block cracking performance, including the use of softer virgin binders and rejuvenators.
- Blending between RAP/RAS and virgin binders is dependent on several factors, including mixing time and temperature as well the RAP/RAS stiffness and RAP/RAS content.

- A limited number of studies have investigated the effect of silo storage on the performance properties of asphalt mixes. The results indicate that the stiffness of the mixes increases with silo storage, and it was generally concluded that additional blending takes place between the recycled and virgin binders inside the silo, increasing the effective binder content.

- The SCB and IDEAL-CT tests are understood to provide a measure of the mix cracking resistance. Both tests were shown to provide good correlation with field performance—including thermal, reflective, and fatigue cracking—based on correlations with the performance of accelerated pavement test sections with 4.5 in. (110 mm) thick asphalt layers at the FHWA accelerated loading facility and a number of other test sections.

- The flexural beam test has been historically validated to correlate with fatigue cracking in the field, when the mix stiffness and fatigue life results are considered in a mechanistic pavement structural analysis.

Key observations from the flexural stiffness and rutting testing include the following:

- Mix A, with 50% RAP and a petroleum-based rejuvenator, and Mix B, with 40% RAP and a soft virgin binder, showed a lower modulus at higher temperatures compared with Mix C, with 20% RAP, 3% RAS, and a soft virgin binder, and Mix D, with 40% RAP and a small amount of biobased rejuvenator. This finding aligned with the HWT and RLT testing, which showed that Mix A and Mix B were more susceptible to rutting.

- The high rejuvenator dose used in Mix A resulted in a low modulus at high temperatures, leading to a reduction in the rutting resistance.

- The use of RAS in Mix C and the use of a low rejuvenator dose in Mix D resulted in a relatively high modulus at high temperatures and increased rutting resistance compared with the other mixes.

- The increase in modulus with silo storage was dependent on the test frequency and the mix design. The maximum increase in stiffness was about 50% to 60% and was noted at low test frequencies (i.e., high temperatures).

- Several parameters were successfully used to measure the rutting resistance of the mixes, including rut depth at 10,000 passes from the HWT, strain at 20,000 cycles from the confined RLT, and flow number and cycles at 5% strain from the unconfined RLT.

- Mix C, which included RAS, showed the best rutting performance while Mix A showed the lowest rutting resistance, possibly due to the use of a high rejuvenator dose.

- The rutting resistance of all the mixes was shown to increase with silo storage, except for the HWT test results for Mix D. The extent of change in rutting parameters varied between mixes and between rutting parameters.

Key observations from the SCB and IDEAL-CT testing include the following:

- The FI from the SCB test and the CT_{index} from the IDEAL-CT test showed strong correlation.

- The cracking resistance of the mixes decreased with silo storage as measured by the FI and CT_{index}.

- The cracking resistance of the mixes was inversely related to the rutting resistance. Mix C, with RAS, had the highest rutting resistance and lowest cracking resistance of all the mixes. On the other hand, Mix B, with 40% RAP and a rejuvenator, showed the lowest rutting resistance and highest cracking resistance of all the mixes.

- The FI was shown to correlate very well with the specimen vertical displacement, particularly the displacement given by the intercept of the post-peak slope. This indicates that the FI can be viewed as a direct measure of the specimen's ability to deform under load.

- The flexural stiffness at 20ºC (68ºF) and 10Hz (E50) showed good correlation with the IDEAL-CT strength, indicating that the IDEAL-CT test can be used to provide a measure of the mix stiffness.

- No correlation was found between the E50 parameter and the CT_{index}. The variability of the air voids of the FI specimens was high, as allowed under the version of the test when the specimens were prepared, which should be considered when interpreting these results. The variability of the air voids contents is not expected to change this conclusion.

Key observations from the flexural beam testing include the following:

- A strain-controlled flexural beam test showed that silo storage led to a reduction in the fatigue life of all mixes at high strain levels and mixed results at low strain levels.

- For all mixes, the strain at which a fatigue life of 250,000 cycles is reached decreased with silo storage.

- No correlation could be established between the cracking parameters—FI and CT_{index}—and the strain at a fatigue life of 250,000 cycles. The variability of the air voids of the FI specimens was high, which should be considered when interpreting these results. The variability of the air voids contents is not expected to change this conclusion.

Key observations from the FAM mix testing include the following:

- Using LAS testing of FAM mixes, the fatigue life of FAM mixes was determined using the VECD model.

- The fatigue life of all FAM mixes decreased with silo storage. Similarly, the strain at which the fatigue life reached 250,000 cycles decreased with silo storage.

- The failure strain, defined as the peak phase angle, also decreased with silo storage for all FAM mixes.

- The failure strain from the FAM mix testing showed good correlation with the strain at 250,000 cycles from the flexural beam test.

- Using temperature-frequency sweep testing of FAM mixes, the modulus master curves of the FAM mixes showed similar ranking of the mixes compared with the modulus master curves of the full-graded mixes. This indicates that FAM mix testing can be used to provide insight into the stiffness of the full-graded mixes.

8.2 Conclusions

The following conclusions are based on the summarized test results:

- The study revealed the significance of silo storage on mix properties. Based on the performance-related testing of full-graded and FAM mixes, silo storage has a notable effect on the properties of high RAP or RAS mixes and the effect is mix dependent. The results also showed that a notable change in mix properties can occur within the first few hours of silo storage (i.e., 5 to 6 hours).

- Cracking tests—the SCB and IDEAL-CT tests—are highly influenced by mix stiffness, which in turn is very sensitive to aging. The IDEAL-CT strength correlated very well with the flexural stiffness of the mix at 20°C (68°F) and 10Hz (E50). The variability of the air void contents of the SCB specimens was high.

- The FI from the SCB test and the CT_{index} from the IDEAL-CT test showed very good correlation. Both parameters appear to provide a good measure of the deformation ability of the mix under monotonic loading.

- The FI and CT_{index} did not directly correlate with four-point flexural beam (4PB) fatigue test results. Most notably, the FI and CT_{index} were not able to capture the poor fatigue performance of Mix A, with high rejuvenator dose and low binder content. Mix A had a low modulus at high temperatures due to the use of a high rejuvenator dose, and the low modulus resulted in a good FI and CT_{index} values. However, Mix A showed poor fatigue performance, possibly due to its low total and virgin binder contents.

- Proper selection of the rejuvenator dose is important to ensure satisfactory performance. Mix A, with a high rejuvenator dose, showed poor fatigue performance and exhibited rutting problems.

- Fatigue testing of FAM mixes showed promising results in terms of characterizing fatigue. However, at this stage, this testing is difficult to implement as a QC/QA test.

- Overall, the interactions of virgin binder grade, RAP content, rejuvenator dose, rejuvenator type, use of RAS, binder content, and silo storage are complex and cannot easily be explained due to conflicting effects and the likelihood of interactions. Performance-related testing provides a means to evaluate the net effects of these mix design and construction variables.

8.3 Recommendations

The following recommendations are made based on the findings from this study:

- The effect of silo storage on the performance properties of high RAP or RAS mixes should be taken into consideration when developing specifications for these types of mixes. The choice of sampling location can significantly change the performance-related testing results. If silo storage is expected to take place during actual production, the recommendation is that mixes be tested for performance-related properties before and after silo storage as part of the job mix formula verification to better capture the range of expected values during production.

- The selection of the rejuvenator dose should not be based only on the manufacturer's recommendations. A systematic procedure that involves optimizing the dose based on performance should be adopted. One such procedure was recently introduced by the NCHRP Project 9-58. A maximum rejuvenator dose should not exceed 8% to 10% of total weight of the binder. The recommendation is also to consider the rejuvenator part of the recycled binder (i.e., the addition of a rejuvenator should not result in using less virgin binder).

- The SCB and IDEAL-CT tests can be used to provide a measure of the mix stiffness using the specimen strength.

- The results presented in this study suggest that the FI and CT_{index} should be used with caution as direct indicators of fatigue performance. Alternatively, the SCB and IDEAL-CT tests may be used to develop a criterion based on the relationship between stiffness and fatigue. Another UCPRC study looked at developing such fatigue criterion based on the testing of a wide range of mixes (*31*).

- Inclusion of medium-term oven-aging procedure to capture some of the effects of the silo storage noted in this study, or in-place aging of the mix when not subjected to silo storage, should be included in future studies.

REFERENCES

1. He, Y., Alavi, Z., Harvey, J., and Jones, D. 2016. "Evaluating Diffusion and Aging Mechanisms in Blending of New and Age-Hardened Binders During Mixing and Paving." *Transportation Research Record* 2574, no. 1: 64–73.

2. Newcomb, D.E., Epps, J.A., and Zhou, F. 2016. *Use of RAP & RAS in High Binder Replacement Asphalt Mixtures: A Synthesis* (Special Report 213). Greenbelt, MD: National Asphalt Pavement Association.

3. Zhou, F., Li, H., Hu, S., Button, J.W., and Epps, J.A. *Characterization and Best Use of Recycled Asphalt Shingles in Hot-Mix Asphalt* (FHWA/TX-13/0-6614-2). College Station, TX: Texas A&M Transportation Institute. static.tti.tamu.edu/tti.tamu.edu/documents/0-6614-2.pdf.

4. Brock, D. 2008. "Maximizing RAP Use." Presented at Summit on Increasing Reclaimed Asphalt Pavement (RAP), Auburn University, Auburn, Alabama.

5. Willis, J.R., Turner, P. Julian, G., Taylor, A.J., Tran, N.H., and F.R.de G. Padula. 2012. *Effects of Changing Virgin Binder Grade and Content on RAP Mixture Properties* (Research Synopsis 12-03). National Center for Asphalt Technology, Auburn University, Auburn, Alabama.

6. Elkashef M., Williams, R.C., and Cochran, E. 2018. "Investigation of Fatigue and Thermal Cracking Behavior of Rejuvenated Reclaimed Asphalt Pavement Binders And Mixtures." *International Journal of Fatigue* 108: 90–95.

7. Yan, Y., Roque, R., Hernando, D., and Chun, S. 2019. "Cracking Performance Characterisation of Asphalt Mixtures Containing Reclaimed Asphalt Pavement With Hybrid Binder." *Road Materials and Pavement Design* 20, no. 2: 347–366.

8. West, R., Kvasnak, A., Tran, N., Powell, B., and Turner, P. 2009. "Testing of Moderate and High Reclaimed Asphalt Pavement Content Mixes: Laboratory And Accelerated Field Performance Testing at the National Center for Asphalt Technology Test Track." *Transportation Research Record* 2126, no. 1: 100–108.

9. West, R.C., Rada, G.R., Willis, J.R., and Marasteanu, M.O. 2013. *Improved Mix Design, Evaluation, and Materials Management Practices for Hot Mix Asphalt with High Reclaimed Asphalt Pavement Content* (Report 752). Washington, DC: Transportation Research Board.

10. McDaniel, R.S., Shah, A., Huber, G.A., and Copeland, A. 2012. "Effects of Reclaimed Asphalt Pavement Content and Virgin Binder Grade on Properties of Plant Produced Mixtures." *Road Materials and Pavement Design* 13, Sup. 1: 161–82.

11. Harvey, J., Monismith, C., Horonjeff, R., Bejarano, M., Tsai, B.W., and Kannekanti, V. 2004. "Long-Life AC Pavements: A Discussion of Design and Construction Criteria based on California Experience." In *International Symposium on Design and Construction of Long Lasting Asphalt Pavements: Proceedings*. Auburn, AL, June 7–9, 2004.

12. Haghshenas, H. 2016. *Research on High-RAP Asphalt Mixtures with Rejuvenators and WMA Additives*. Lincoln, NE: Nebraska Transportation Center. digitalcommons.unl.edu/cgi/viewcontent.cgi?article=1158 &context=ndor.

13. Zaumanis, M., Mallick, R.B., Poulikakos, L., and Frank, R. 2014. "Influence of Six Rejuvenators on the Performance Properties of Reclaimed Asphalt Pavement (RAP) Binder and 100% Recycled Asphalt Mixtures." *Construction and Building Materials* 71: 538–550.

14. McDaniel, R., and Anderson, R.M. 2001. *Recommended Use of Reclaimed Asphalt Pavement in the Superpave Mixture Design Method* (NCHRP Report 452). Washington, DC: Transportation Research Board. onlinepubs.trb.org/onlinepubs/nchrp/nchrp_rpt_452.pdf.

15. He, Y., Alavi, Z., Harvey, J., and Jones, D. 2016. "Evaluating Diffusion and Aging Mechanisms in Blending of New and Age-Hardened Binders During Mixing and Paving." *Transporation Research Record* 2574, no. 1: 64–73.

16. Kriz, P., Grant, D.L., Veloza, B.A., Gale, M.J., Blahey, A.G., Brownie, J.H., Shirts, R.D., and Maccarrone, S. 2014. "Blending and Diffusion of Reclaimed Asphalt Pavement and Virgin Asphalt Binders." *Road Materials and Pavement Design* 15, Sup. 1: 78–112.

17. Jacques, C., Daniel, J.S., Bennert, T., Reinke, G., Norouzi, A., Ericson, C., Mogawer, W., and Kim, Y.R. 2016. "Effect of Silo Storage Time on the Characteristics of Virgin and Reclaimed Asphalt Pavement Mixtures." *Transportation Research Record* 2573, no. 1: 76–85.

18. Kriz, P., Grant, D.L., Gale, M.J., Lavorato, S., and Pahalan, A. 2014. "Reclaimed Asphalt Pavement-Virgin Binder Diffusion In Asphalt Mixes." In *Proceedings of the Fifty-Ninth Annual Conference of the Canadian Technical Asphalt Association (CTAA)*. Winnipeg, Manitoba, Canada, November 15-19, 2014.

19. Kadhim, H., and Baaj, H. 2020. "Evaluating the Performance of the Asphalt Mixes Containing Reclaimed Asphalt Pavement by Considering the Effect of Silo Storage Time." *Journal of Testing and Evaluation*, American Society of Testing and Materials 48, no. 1.

20. Kadhim, H., and Baaj, H. 2018. "Evaluation of the Impact of Silo Storage on Thermal Cracking of the Hot Mix Asphalt with RAP." Presented at TAC 2018: Innovation and Technology, Evolving Transportation, Transportation Associate of Canada Conference and Exhibition, September 30–October 3, 2018, Saskatoon, Saskatchewan, Canada. tac-atc.ca/sites/default/files/conf_papers/kadhimh-evaluation_of_the_impact.pdf.

21. Zhou, F., Newcomb, D., Gurganus, C., Banihashemrad, S., Park, E.S., Sakhaeifar, M., Park; E.S., and Lytton, R.L. 2016. *Experimental Design for Field Validation of Laboratory Tests to Assess Cracking Resistance of Asphalt Mixtures*. Washington, D.C.: Transportation Research Board.

22. Ozer, H., Al-Qadi, I.L., Lambros, J., El-Khatib, A., Singhvi, P., and Doll, B. 2016. "Development of the Fracture-Based Flexibility Index for Asphalt Concrete Cracking Potential Using Modified Semi-Circle Bending Test Parameters." *Construction and Building Materials* 115: 390–401.

23. Zhou, F., Im, S., Sun, L., and Scullion, T. 2017. "Development of an IDEAL Cracking Test for Asphalt Mix Design and QC/QA." *Road Materials and Pavement Design* 18, Sup. 4: 405–427.

24. Chen, C. 2020. "Validation of Laboratory Cracking Tests for Field Top-Down Cracking Performance." PhD diss., Auburn University. etd.auburn.edu/xmlui/handle/10415/7135.

25. Ozer, H., Al-Qadi, I.L., Singhvi, P., Bausano, J., Carvalho, R., Li, X., and Nelson, G. 2018. "Prediction of Pavement Fatigue Cracking at an Accelerated Testing Section Using Asphalt Mixture Performance Tests." *International Journal of Pavement Engineering* 19: 264–278.

26. Harvey, J., Lee, T., Sousa, J., Pak, J., and Monismith, C.L. 1994. "Evaluation of Fatigue and Permanent Deformation Properties of Several Asphalt-Aggregate Field Mixes Using Strategic Highway Research Program A-003A Equipment." *Transportation Research Record* 1454: 123–133. onlinepubs.trb.org /Onlinepubs/trr/1994/1454/1454-015.pdf.

27. Alavi, Z., He, Y., Harvey, J., and Jones, D. 2015. *Evaluation of the Combined Effects of Reclaimed Asphalt Pavement (RAP), Reclaimed Asphalt Shingles (RAS), and Different Virgin Binder Sources on the Performance of Blended Binders for Mixes with Higher Percentages of RAP and RAS* (UCPRC-RR-2015-06). Davis and Berkeley, CA: University of California Pavement Research Center. escholarship.org/uc/item/1hg4p0pr.

28. Elkashef, M, Hung, S.S., Jones, D., and Harvey, J. 2019. "Using Predictive Models to Estimate the Properties of Binders in Reclaimed Asphalt Pavement Mixes using Fine Aggregate Matrix Mix Testing." *Transportation Research Record* 2673, no. 6: 501–511.

29. Schapery, R.A. 1984. "Correspondence Principles and a Generalized J Integral for Large Deformation and Fracture Analysis of Viscoelastic Media." *International Journal of Fracture* 25: 195–223.

30. Hintz, C., Velasquez, R., Johnson, C., and Bahia, H. 2011. "Modification and Validation of Linear Amplitude Sweep Test for Binder Fatigue Specification." Transportation Research Record: Journal of the Transportation Research Board 2207, no. 1: 99–106.

31. Jiao, L., Harvey, J., Wu, R., Elkashef, M., Jones, D., and Liang, Y. 2023. *Preliminary Study on Developing a Surrogate Performance-Related Test for Cracking of Asphalt Pavements* (UCPRC-RR-2021-02). Davis and Berkeley, CA: University of California Pavement Research Center. escholarship.org/uc/item/52d1d1q5.